

A coupled multipoint stress - multipoint flux mixed finite element method for the Biot poroelasticity model

Ilona Ambartsumyan^{*†}

Eldar Khattatov^{*†}

Ivan Yotov^{*}

August 16, 2019

Abstract

In this work we present a mixed finite element method for a five-field formulation of the Biot system of poroelasticity that reduces to cell-centered finite differences for pressure and displacement on simplicial and quadrilateral grids. A mixed stress-displacement-rotation formulation for elasticity with weak stress symmetry is coupled with a mixed velocity-pressure Darcy formulation. The spatial discretization is based on combining the multipoint flux mixed finite element (MFMFE) method for Darcy flow and the multipoint stress mixed finite element (MSMFE) method for elasticity. It uses the lowest order Brezzi-Douglas-Marini mixed finite element spaces for the Darcy velocity and poroelastic stress, piecewise constant pressure and displacement, and continuous piecewise linear or bilinear rotation. A vertex quadrature rule is applied to the velocity, stress, and stress-rotation bilinear forms, which block-diagonalizes the corresponding matrices and allows for local velocity, stress, and rotation elimination. This leads to a cell-centered symmetric and positive-definite system for pressure and displacement at each time step. We perform error analysis for the semidiscrete formulation, establishing first order convergence for all variables in their natural norms. The numerical tests confirm the theoretical convergence rates and illustrate the locking-free property of the method.

1 Introduction

Geoscience applications such as environmental cleanup, petroleum production, solid waste disposal, and carbon sequestration are inherently coupled with field phenomena such as surface subsidence, uplift displacement, pore collapse, cavity generation, hydraulic fracturing, thermal fracturing, wellbore collapse, sand production, and fault activation. This coupled nature of fluid motion through porous media and solid deformation makes it challenging for numerical modeling and simulation.

In this work we use is the classical Biot consolidation system in poroelasticity [8, 36] under a quasi-static assumption as the mathematical model for such coupled fluid-solid system. The system of equations consists of an equilibrium equation for the solid and a mass balance equation for the fluid. The contribution of the fluid pressure to the total stress of the solid, and the divergence of the solid displacement represents an additional term in the fluid content. Numerical modeling of this coupled system is well studied in the literature. In [26, 27], Taylor-Hood finite elements are employed for a displacement-pressure variational formulation. A least squares formulation that approximates directly the solid stress and the fluid velocity is studied in [22, 23]. Finite difference schemes on staggered grids designed to avoid nonphysical oscillations at early times have been developed in 1D in [16, 19]. The method in [16] can handle discontinuous coefficients through harmonic averaging. A formulation based on mixed finite element (MFE) methods for flow and continuous Galerkin (CG) for elasticity has been proposed in [30, 31]. The coupled multipoint flux mixed finite element method (MFMFE) for flow and CG method for elasticity has been studied in [42]. On the other hand, as the MFE methods

^{*}Department of Mathematics, University of Pittsburgh, Pittsburgh, PA 15260, USA; {ila6@pitt.edu, elk58@pitt.edu, yotov@math.pitt.edu}. Partially supported by DOE grant DE-FG02-04ER25618 and NSF grants DMS 1418947 and DMS 1818775.

[†]Oden Institute for Computational Engineering and Sciences, The University of Texas at Austin, Austin, TX 78712, USA; {ailona@austin.utexas.edu, ekhattatov@austin.utexas.edu}.

for elasticity become more popular in the finite element community, the five-field MFE formulation for the Biot system was presented in [24]. The advantages of this approach is that the fluid and mechanics approximations are locally mass conservative and the fluid velocity and poroelastic stress are computed directly. Moreover, this approach guarantees robustness and locking-free properties with respect to physical parameters. In [20], a parallel domain decomposition method has been developed for coupling a time-dependent poroelastic model in a localized region with an elastic model in adjacent regions. Each model is discretized independently on nonmatching grids and the systems are coupled using DG jumps and mortars. Applications of the Biot system to the computational modeling of coupled reservoir flow and geomechanics can be found in [12, 17, 18, 35].

The focus of this paper is to develop a discretization method for the poroelasticity system in the mixed form that is suitable for irregular and rough grids, discontinuous full tensor permeabilities and Lamé coefficients that are often encountered in modeling subsurface flows. To this end, we develop a formulation that couples multipoint flux mixed finite element (MFMFE) methods for flow with multipoint stress mixed finite element (MSMFE) methods for elasticity. The MFMFE method was developed for Darcy flow in [21, 43, 40]. It is locally conservative with continuous fluxes and can be viewed within a variational framework as a mixed finite element method with special approximating spaces and quadrature rules. The MFMFE method allows for an accurate and efficient treatment of irregular geometries and heterogeneities such as faults, layers, and pinchouts that require highly distorted grids and discontinuous coefficients. The resulting discretizations are cell-centered with convergent pressures and velocities on general hexahedral and simplicial grids. The reader is referred to [39] for the performance of the MFMFE method for flow on a benchmark test using rough 3D grids and anisotropic coefficients. Similarly, the MSMFE method was developed in [3, 4] and shares the same locality properties with continuous normal stresses. The method is also derived within an variational framework as a mixed finite element method for elasticity with weak symmetry using special approximating spaces and quadrature rules.

As the MFMFE method was motivated by the multipoint flux approximation (MPFA) methods [2, 1, 14, 15], the MSMFE method was motivated by the multipoint stress approximation (MPSA) [28]. Both frameworks allow for local flux and stress elimination around grid vertices and reduction to a cell-centered pressure and displacement scheme, respectively. The coupled scheme based on MPSA and MPFA methods for the elasticity and flow parts of the Biot system was proposed in [29]. Similar elimination is achieved in the MFMFE and MSMFE variational framework, by employing appropriate finite element spaces and special quadrature rules. Both methods are based on the BDM_1 [10] spaces with a trapezoidal quadrature rule applied on the reference element, [21, 43, 40]. Our goal in this paper is to emphasize the applicability of the MSMFE method for solid mechanics in the Biot system, which, together with the MFMFE method used for the flow part of the model will result in an efficient technique for solving a coupled saddle-point type problem.

In this paper, we develop convergence analysis for the MFMFE-MSMFE numerical approximation of the time-dependent poroelasticity system. We study the symmetric version of the MFMFE and MSMFE methods on simplicial grids in 2 and 3 dimensions and quadrilateral grids. Theoretical and numerical results demonstrate first-order convergence in time and space for the fluid pressure and velocity, as well as for the poroelastic stress, solid displacement and rotation.

The rest of the paper is organized as follows. The problem formulation and the numerical approximation are presented in Section 2. Well-posedness of the proposed coupled MFMFE-MSMFE method is studied in Section 3. Section 4 shows the reduction of the method to the cell-centered finite difference (CCFD) scheme. The convergence analysis for the continuous in time scheme is developed in Sections 5. Finally, Section 6 is devoted to computational experiments

2 Model problem and a fully mixed weak formulation

In this section we describe the poroelasticity system and its fully mixed formulation based on a weak stress symmetry. Let Ω be a simply connected bounded domain of \mathbb{R}^d , $d = 2, 3$, occupied by a poroelastic media saturated with fluid. Let \mathbb{M} , \mathbb{S} , and \mathbb{N} be the spaces of real $d \times d$ matrices, symmetric matrices, and skew-symmetric matrices, respectively. The divergence operator $\text{div} : \mathbb{R}^d \rightarrow \mathbb{R}$ is the

usual divergence for vector fields. It also acts on matrix fields, $\text{div} : \mathbb{M} \rightarrow \mathbb{R}^d$ by applying the divergence row-wise. The operator $\text{curl} : \mathbb{R}^3 \rightarrow \mathbb{R}^3$ is the usual curl when applied to vector fields in three dimensions. In two dimensions, it acts on scalar fields, $\text{curl} : \mathbb{R} \rightarrow \mathbb{R}^2$, defined as

$$\text{curl} \phi = (\partial_2 \phi, -\partial_1 \phi).$$

The action of the curl operator on vector fields in two dimensions, $\text{curl} : \mathbb{R}^2 \rightarrow \mathbb{M}$, and matrix fields in three dimensions, $\text{curl} : \mathbb{M} \rightarrow \mathbb{M}$, produces a matrix field by acting row-wise.

The stress-strain constitutive relationship for the poroelastic body is

$$A\sigma_e = \epsilon(u), \quad (2.1)$$

where at each point $x \in \Omega$, $A(x) : \mathbb{S} \rightarrow \mathbb{S}$, extendable to $A(x) : \mathbb{M} \rightarrow \mathbb{M}$, is a symmetric, bounded and uniformly positive definite linear operator representing the compliance tensor, σ_e is the elastic stress, u is the solid displacement, and $\epsilon(u) = \frac{1}{2}(\nabla u + \nabla u^T)$. In the case of a homogeneous and isotropic body,

$$A\sigma = \frac{1}{2\mu} \left(\sigma - \frac{\lambda}{2\mu + d\lambda} \text{tr}(\sigma)I \right),$$

where I is the $d \times d$ identity matrix and $\mu > 0, \lambda \geq 0$ are the Lamé coefficients. In this case the elastic stress is $\sigma_e = 2\mu\epsilon(u) + \lambda \text{div} u I$. The poroelastic stress, which includes the effect of the fluid pressure p , is given as

$$\sigma = \sigma_e - \alpha p I, \quad (2.2)$$

where $0 < \alpha \leq 1$ is the Biot-Willis constant.

Given a vector field f representing the body forces and a source term q , the quasi-static Biot system [8] that governs the fluid flow within the poroelastic media is as follows:

$$-\text{div} \sigma = f \quad \text{in } \Omega \times (0, T], \quad (2.3)$$

$$K^{-1}z + \nabla p = 0 \quad \text{in } \Omega \times (0, T], \quad (2.4)$$

$$\frac{\partial}{\partial t}(c_0 p + \alpha \text{div} u) + \text{div} z = q \quad \text{in } \Omega \times (0, T], \quad (2.5)$$

where z is the Darcy velocity, $c_0 > 0$ is a mass storativity coefficient, and K is a symmetric and positive definite tensor representing the permeability of the porous media divided by the fluid viscosity. The system is closed with the boundary conditions

$$u = g_u \quad \text{on } \Gamma_D^{displ} \times (0, T], \quad \sigma n = 0 \quad \text{on } \Gamma_N^{stress} \times (0, T], \quad (2.6)$$

$$p = g_p \quad \text{on } \Gamma_D^{pres} \times (0, T], \quad z \cdot n = 0 \quad \text{on } \Gamma_N^{vel} \times (0, T], \quad (2.7)$$

and the initial conditions $p(x, 0) = p_0(x)$, $u(x, 0) = u_0(x)$ in Ω , where $\Gamma_D^{displ} \cup \Gamma_N^{stress} = \Gamma_D^{pres} \cup \Gamma_N^{vel} = \partial\Omega$ and n is the outward unit normal vector field on $\partial\Omega$. We assume for simplicity that $|\Gamma_D^*| > 0$, for $* = \{displ, pres\}$. The well posedness of the above system has been studied in [36].

Throughout the paper, C denotes a generic positive constant that is independent of the discretization parameter h . We will also use the following standard notation. For a domain $G \subset \mathbb{R}^d$, the $L^2(G)$ inner product and norm for scalar, vector, or tensor valued functions are denoted $(\cdot, \cdot)_G$ and $\|\cdot\|_G$, respectively. The norms and seminorms of the Sobolev spaces $W^{k,p}(G)$, $k \in \mathbb{R}, p > 0$ are denoted by $\|\cdot\|_{k,p,G}$ and $|\cdot|_{k,p,G}$, respectively. The norms and seminorms of the Hilbert spaces $H^k(G)$ are denoted by $\|\cdot\|_{k,G}$ and $|\cdot|_{k,G}$, respectively. We omit G in the subscript if $G = \Omega$. For a section of the domain or element boundary $S \subset \mathbb{R}^{d-1}$ we write $\langle \cdot, \cdot \rangle_S$ and $\|\cdot\|_S$ for the $L^2(S)$ inner product (or duality pairing) and norm, respectively. We will also use the spaces

$$H(\text{div}; \Omega) = \{v \in L^2(\Omega, \mathbb{R}^d) : \text{div} v \in L^2(\Omega)\},$$

$$H(\text{div}; \Omega, \mathbb{M}) = \{\tau \in L^2(\Omega, \mathbb{M}) : \text{div} \tau \in L^2(\Omega, \mathbb{R}^d)\},$$

equipped with the norm

$$\|\tau\|_{\text{div}} = (\|\tau\|^2 + \|\text{div } \tau\|^2)^{1/2}.$$

We next present the mixed weak formulation, which has been proposed in [24]. Using (2.1) and (2.2), we have

$$\text{div } u = \text{tr}(\epsilon(u)) = \text{tr}(A\sigma_e) = \text{tr } A(\sigma + \alpha p I),$$

which can be substituted in (2.5) to give

$$\partial_t(c_0 p + \alpha \text{tr } A(\sigma + \alpha p I)) + \text{div } z = q.$$

In the weakly symmetric stress formulation, we allow for σ to be non-symmetric and introduce the Lagrange multiplier $\gamma = \text{Skew}(\nabla u)$, $\text{Skew}(\tau) = \frac{1}{2}(\tau - \tau^T)$, from the space of skew-symmetric matrices. The constitutive equation (2.1) can be rewritten as

$$A(\sigma + \alpha p I) = \nabla u - \gamma.$$

The mixed weak formulation of the Biot problem reads: find $(\sigma, u, \gamma, z, p) \in W^{1,\infty}(0, T; \mathbb{X}) \times L^\infty(0, T; V) \times L^\infty(0, T; \mathbb{Q}) \times L^\infty(0, T; Z) \times W^{1,\infty}(0, T; W)$ such that $\sigma(0) = A^{-1}\epsilon(u_0) - \alpha p_0 I$, $p(0) = p_0$, and

$$(A(\sigma + \alpha p I), \tau) + (u, \text{div } \tau) + (\gamma, \tau) = \langle g_u, \tau n \rangle_{\Gamma_D^{\text{displ}}}, \quad \forall \tau \in \mathbb{X}, \quad (2.8)$$

$$(\text{div } \sigma, v) = -(f, v), \quad \forall v \in V, \quad (2.9)$$

$$(\sigma, \xi) = 0, \quad \forall \xi \in \mathbb{Q}, \quad (2.10)$$

$$(K^{-1}z, \zeta) - (p, \text{div } \zeta) = -\langle g_p, \zeta \cdot n \rangle_{\Gamma_D^{\text{pres}}}, \quad \forall \zeta \in Z, \quad (2.11)$$

$$c_0(\partial_t p, w) + \alpha(\partial_t A(\sigma + \alpha p I), wI) + (\text{div } z, w) = (q, w), \quad \forall w \in W, \quad (2.12)$$

where we have used the identity $(\text{tr } A\tau, w) = (A\tau, wI)$ and the functional spaces are defined as

$$\begin{aligned} \mathbb{X} &= \{\tau \in H(\text{div}; \Omega, \mathbb{M}) : \tau n = 0 \text{ on } \Gamma_N^{\text{stress}}\}, & V &= L^2(\Omega, \mathbb{R}^d), & \mathbb{Q} &= L^2(\Omega, \mathbb{N}), \\ Z &= \{\zeta \in H(\text{div}; \Omega, \mathbb{R}^d) : \zeta \cdot n = 0 \text{ on } \Gamma_N^{\text{vel}}\}, & W &= L^2(\Omega). \end{aligned}$$

3 Mixed finite element discretization

We begin with the discretization of the fully mixed weak formulation of the poroelasticity system (2.8)–(2.12), based on mixed finite element methods for elasticity and Darcy flow. We then present the multipoint stress - multipoint flux mixed finite element method, which employs the vertex quadrature rule for the stress, rotation, and velocity bilinear forms and can be reduced to a symmetric and positive definite cell centered system for displacement and pressure only.

3.1 Mixed finite element spaces

We next present the MFE discretization of (2.8)–(2.12). For simplicity, assume that Ω is a polygonal domain. Let \mathcal{T}_h be a shape-regular and quasi-uniform [13] finite element partition of Ω , consisting of triangles and/or quadrilaterals in two dimensions and tetrahedra in three dimensions. Let $h = \max_{E \in \mathcal{T}_h} \text{diam}(E)$. For any element $E \in \mathcal{T}_h$ there exists a bijection mapping $F_E : \hat{E} \rightarrow E$, where \hat{E} is a reference element. We denote the Jacobian matrix by DF_E and let $J_E = |\det(DF_E)|$. We note that the mapping is affine with constant DF_E in the case of simplicial elements and bilinear with linear DF_E in the case of quadrilaterals. The shape-regularity and quasiuniformity of the grids imply that

$$\|DF_E\|_{0,\infty,\hat{E}} \sim h, \quad \|J_E\|_{0,\infty,\hat{E}} \sim h^d \quad \forall E \in \mathcal{T}_h. \quad (3.1)$$

Let $\mathbb{X}_h \times V_h \times \mathbb{Q}_h$ be the triple $(\mathcal{BDM}_1)^d \times (\mathcal{P}_0)^d \times (\mathcal{P}_1^{\text{cts}})^{d \times d, \text{skew}}$ on simplicial elements or $(\mathcal{BDM}_1)^d \times (\mathcal{Q}_0)^d \times (\mathcal{Q}_1^{\text{cts}})^{d \times d, \text{skew}}$ on quadrilaterals, where \mathcal{P}_k denotes the space of polynomials of total degree k and \mathcal{Q}_k denotes the space of polynomials of degree k in each variable. These spaces are

modifications of the lowest order Arnold-Falk-Winther spaces on simplices [7] and the related Arnold-Awanou-Qiu spaces on quadrilaterals [5], which have constant rotations. The triple $\mathbb{X}_h \times V_h \times \mathbb{Q}_h$ with continuous linear or mapped bilinear rotations we consider here has been shown to be inf-sup stable for mixed elasticity with weak stress symmetry in [9] on simplices and in [4] on quadrilaterals. For the Darcy flow discretization we consider $Z_h \times W_h$ to be the lowest order $\mathcal{BDM}_1 \times \mathcal{P}_0$ MFE spaces [10, 11]. On the reference simplex, these spaces are defined as

$$\hat{\mathbb{X}}(\hat{E}) = \left(\mathcal{P}_1(\hat{E})^d \right)^d, \quad \hat{V}(\hat{E}) = \mathcal{P}_0(\hat{E})^d, \quad \hat{\mathbb{Q}}(\hat{E}) = \mathcal{P}_1(\hat{E})^{d \times d, skew}, \quad (3.2)$$

$$\hat{Z}(\hat{E}) = \mathcal{P}_1(\hat{E})^d, \quad \hat{W}(\hat{E}) = \mathcal{P}_0(\hat{E}). \quad (3.3)$$

On the reference square, the spaces are defined as

$$\begin{aligned} \hat{\mathbb{X}}(\hat{E}) &= \left(\mathcal{P}_1(\hat{E})^2 + r \operatorname{curl}(\hat{x}^2 \hat{y}) + s \operatorname{curl}(\hat{x} \hat{y}^2) \right)^2 \\ &= \begin{pmatrix} \alpha_1 \hat{x} + \beta_1 \hat{y} + \gamma_1 + r_1 \hat{x}^2 + 2s_1 \hat{x} \hat{y} & \alpha_2 \hat{x} + \beta_2 \hat{y} + \gamma_2 - 2r_1 \hat{x} \hat{y} - s_1 \hat{y}^2 \\ \alpha_3 \hat{x} + \beta_3 \hat{y} + \gamma_3 + r_2 \hat{x}^2 + 2s_2 \hat{x} \hat{y} & \alpha_4 \hat{x} + \beta_4 \hat{y} + \gamma_4 - 2r_2 \hat{x} \hat{y} - s_2 \hat{y}^2 \end{pmatrix}, \\ \hat{V}(\hat{E}) &= \mathcal{P}_0(\hat{E})^d, \quad \hat{\mathbb{Q}}(\hat{E}) = \mathcal{Q}_1(\hat{E})^{2 \times 2, skew}, \\ \hat{Z}(\hat{E}) &= \mathcal{P}_1(\hat{E})^2 + r \operatorname{curl}(\hat{x}^2 \hat{y}) + s \operatorname{curl}(\hat{x} \hat{y}^2) = \begin{pmatrix} \alpha_5 \hat{x} + \beta_5 \hat{y} + \gamma_5 + r_3 \hat{x}^2 + 2s_3 \hat{x} \hat{y} \\ \alpha_6 \hat{x} + \beta_6 \hat{y} + \gamma_6 - 2r_3 \hat{x} \hat{y} - s_3 \hat{y}^2 \end{pmatrix}, \\ \hat{W}(\hat{E}) &= \mathcal{P}_0(\hat{E}). \end{aligned} \quad (3.4)$$

These spaces satisfy

$$\operatorname{div} \hat{\mathbb{X}}(\hat{E}) = \hat{V}(\hat{E}), \operatorname{div} \hat{Z}(\hat{E}) = \hat{W}(\hat{E}); \quad \forall \hat{\tau} \in \hat{\mathbb{X}}(\hat{E}), \forall \hat{\zeta} \in \hat{Z}(\hat{E}), \forall \hat{e} \in \partial \hat{E}, \quad \hat{\tau} \cdot \hat{n}_{\hat{e}} \in \mathcal{P}_1(\hat{e})^d, \quad \hat{\zeta} \cdot \hat{n}_{\hat{e}} \in \mathcal{P}_1(\hat{e}).$$

It is known [10, 11] that the degrees of freedom for \mathcal{BDM}_1 can be chosen to be the values of the normal fluxes at any two points on each edge \hat{e} of \hat{E} in 2d or any three points one each face \hat{e} of \hat{E} in 3d. reference tetrahedron, and similarly for the normal stresses in the case of $(\mathcal{BDM}_1)^d$. Here we choose these points to be at the vertices of \hat{e} for both the velocity and stress spaces. This choice is motivated by the use of the vertex quadrature rule introduced in the next section.

To define the above spaces on any physical element $E \in \mathcal{T}_h$, the following transformations are used

$$\begin{aligned} \tau &\xleftrightarrow{\mathcal{P}} \hat{\tau} : \tau^T = \frac{1}{J_E} DF_E \hat{\tau}^T \circ F_E^{-1}, & v &\leftrightarrow \hat{v} : v = \hat{v} \circ F_E^{-1}, & \xi &\leftrightarrow \hat{\xi} : \xi = \hat{\xi} \circ F_E^{-1}, \\ \zeta &\xleftrightarrow{\mathcal{P}} \hat{\zeta} : \zeta = \frac{1}{J_E} DF_E \hat{\zeta} \circ F_E^{-1}, & w &\leftrightarrow \hat{w} : w = \hat{w} \circ F_E^{-1}, \end{aligned}$$

for $\tau \in \mathbb{X}$, $v \in V$, $\xi \in \mathbb{Q}$, $\zeta \in Z$ and $w \in W$. The velocity vector and stress tensor are mapped by the Piola transformation, where the stress is transformed row-wise. The Piola transformation preserves the normal components and the divergence of the stress and velocity on element edges or faces. In particular, it can be shown that

$$\tau n_e = \frac{1}{|J_E DF^{-T} \hat{n}_{\hat{e}}|_{\mathbb{R}^d}} \hat{\tau} \cdot \hat{n}_{\hat{e}}, \quad \zeta \cdot n_e = \frac{1}{|J_E DF^{-T} \hat{n}_{\hat{e}}|_{\mathbb{R}^d}} \hat{\zeta} \cdot \hat{n}_{\hat{e}}, \quad \operatorname{div} \tau = \frac{1}{J_E} \operatorname{div} \hat{\tau}, \quad \operatorname{div} \zeta = \frac{1}{J_E} \operatorname{div} \hat{\zeta},$$

where $|\cdot|_{\mathbb{R}^d}$ denotes the Euclidean vector norm. The finite element spaces on \mathcal{T}_h are defined as

$$\begin{aligned} \mathbb{X}_h &= \{ \tau \in \mathbb{X} : \tau|_E \xleftrightarrow{\mathcal{P}} \hat{\tau}, \hat{\tau} \in \hat{\mathbb{X}}(\hat{E}) \quad \forall E \in \mathcal{T}_h \}, \\ V_h &= \{ v \in V : v|_E \leftrightarrow \hat{v}, \hat{v} \in \hat{V}(\hat{E}) \quad \forall E \in \mathcal{T}_h \}, \\ \mathbb{Q}_h &= \{ \xi \in H^1(\Omega, \mathbb{N}) : \xi|_E \leftrightarrow \hat{\xi}, \hat{\xi} \in \hat{\mathbb{Q}}(\hat{E}) \quad \forall E \in \mathcal{T}_h \}, \\ Z_h &= \{ \zeta \in Z : \zeta|_E \xleftrightarrow{\mathcal{P}} \hat{\zeta}, \hat{\zeta} \in \hat{Z}(\hat{E}) \quad \forall E \in \mathcal{T}_h \}, \\ W_h &= \{ w \in W : w|_E \leftrightarrow \hat{w}, \hat{w} \in \hat{W}(\hat{E}) \quad \forall E \in \mathcal{T}_h \}. \end{aligned} \quad (3.5)$$

3.2 The coupled \mathcal{BDM}_1 mixed finite element method

With the finite element spaces defined above, the semidiscrete five-field mixed finite element approximation of the Biot poroelasticity system (2.8)–(2.12) reads as follows: find $(\sigma_h, u_h, \gamma_h, z_h, p_h) \in W^{1,\infty}(0, T; \mathbb{X}_h) \times L^\infty(0, T; V_h) \times L^\infty(0, T; \mathbb{Q}_h) \times L^\infty(0, T; Z_h) \times W^{1,\infty}(0, T; W_h)$ such that

$$(A(\sigma_h + \alpha p_h I), \tau) + (u_h, \operatorname{div} \tau) + (\gamma_h, \tau) = \langle g_u, \tau n \rangle_{\Gamma_D^{displ}}, \quad \forall \tau \in \mathbb{X}_h, \quad (3.6)$$

$$(\operatorname{div} \sigma_h, v) = -(f, v), \quad \forall v \in V_h, \quad (3.7)$$

$$(\sigma_h, \xi) = 0, \quad \forall \xi \in \mathbb{Q}_h, \quad (3.8)$$

$$(K^{-1} z_h, \zeta) - (p_h, \operatorname{div} \zeta) = -\langle g_p, \zeta \cdot n \rangle_{\Gamma_D^{pres}}, \quad \forall \zeta \in Z_h, \quad (3.9)$$

$$c_0 (\partial_t p_h, w) + \alpha (\partial_t A(\sigma_h + \alpha p_h I), wI) + (\operatorname{div} z_h, w) = (q, w), \quad \forall w \in W_h, \quad (3.10)$$

with initial conditions $\sigma_h(0)$ and $p_h(0)$ suitable approximations of $A^{-1}\epsilon(u_0) - \alpha p_0 I$ and p_0 , respectively. The above method is studied in [24], where it is shown that the method is robust for small storage coefficient and for nearly incompressible materials. However, with an implicit time discretization, it requires the solution of a large five-field saddle point system at each time step. Motivated by the MFMFE [43] and MSMFE [3, 4] methods, in the next sections we develop a coupled MSMFE-MFMFE method based on a vertex quadrature rule that allows for local elimination of the stress, rotation, and velocity, resulting in a symmetric and positive-definite cell-centered displacement-pressure system.

3.3 A quadrature rule

For any element-wise continuous vector or tensor functions ϕ and ψ on Ω , we denote by

$$(\phi, \psi)_Q = \sum_{E \in \mathcal{T}_h} (\phi, \psi)_{Q,E}$$

the application of the element-wise vertex quadrature rule for computing (ϕ, ψ) . The integration on any element E is performed by mapping to the reference element \hat{E} . Let $\tilde{\phi}$ and $\tilde{\psi}$ be the mapped functions on \hat{E} , using the standard change of variables. Since $(\phi, \psi)_E = (\tilde{\phi}, \tilde{\psi} J_E)_{\hat{E}}$, we define

$$(\phi, \psi)_{Q,E} = \frac{|\hat{E}|}{s} \sum_{i=1}^s \tilde{\phi}(\hat{\mathbf{r}}_i) \cdot \tilde{\psi}(\hat{\mathbf{r}}_i) J_E(\hat{\mathbf{r}}_i) = \frac{|\hat{E}|}{s} \sum_{i=1}^s \phi(\mathbf{r}_i) \cdot \psi(\mathbf{r}_i) J_E(\hat{\mathbf{r}}_i),$$

where s is the number of vertices of E , \mathbf{r}_i and $\hat{\mathbf{r}}_i$, $i = 1, \dots, s$, are the vertices of E and \hat{E} , respectively, and \cdot has a meaning of inner product for both vector and tensor valued functions.

The quadrature rule will be applied to the velocity, stress, and stress-rotation bilinear forms. All three variables have degrees of freedom associated with the mesh vertices. The quadrature rule decouples degrees of freedom associated with a vertex from the rest of the degrees of freedom, resulting in block-diagonal matrices corresponding to these bilinear forms. Therefore the velocity, stress, and rotation can be locally eliminated, reducing the method to solving a cell-centered pressure-displacement system. More details on this reduction will be provided in the following sections.

The analysis of the MSMFE-MFMFE method will utilize the following continuity and coercivity properties of the quadrature bilinear forms.

Lemma 3.1. *There exist positive constants C_1 and C_2 independent of h , such that for any linear uniformly bounded and positive-definite operator L and for all $\phi, \psi \in \mathbb{X}_h, \mathbb{Q}_h, Z_h, W_h$,*

$$(L\phi, \phi)_Q \geq C_1 \|\phi\|^2, \quad (L\phi, \psi)_Q \leq C_2 \|\phi\| \|\psi\|. \quad (3.11)$$

Proof. The proof for functions in $\mathbb{X}_h, \mathbb{Q}_h, Z_h$ has been shown in [43, 3, 4]. The proof for functions in W_h is similar. \square

Lemma 3.1 implies the following norm equivalence.

Corollary 3.1. *$(L\phi, \phi)_Q^{1/2}$ is a norm equivalent to $\|\phi\|$, which will be denoted by $\|L^{1/2}\phi\|_Q$.*

3.4 The coupled multipoint stress-multipoint flux mixed finite element method

We first note that there is a slight difference in the incorporation of the Dirichlet boundary conditions between the simplicial and quadrilateral grids. In particular, in the case of quadrilaterals, the L^2 projection of the boundary data onto the space of piecewise constants must be used in order to obtain optimal approximation of the boundary term. On the other hand, such projection should not be used on simplices, since it would result in non-optimal approximation. The difference is due to different properties of the quadrature rules on simplicial and quadrilateral grids, see [41, 3, 4]. For the conformity and simplicity of the presentation, for the rest of the paper we consider $g_u = g_p = 0$.

Our method, referred to as the MSMFE-MFMFE method, in its semidiscrete form is defined as follows: find $(\sigma_h, u_h, \gamma_h, z_h, p_h) \in W^{1,\infty}(0, T; \mathbb{X}_h) \times L^\infty(0, T; V_h) \times L^\infty(0, T; \mathbb{Q}_h) \times L^\infty(0, T; Z_h) \times W^{1,\infty}(0, T; W_h)$ such that $\sigma_h(0)$ and $p_h(0)$ are given and

$$(A(\sigma_h + \alpha p_h I), \tau)_Q + (u_h, \operatorname{div} \tau) + (\gamma_h, \tau)_Q = 0, \quad \forall \tau \in \mathbb{X}_h, \quad (3.12)$$

$$(\operatorname{div} \sigma_h, v) = -(f, v), \quad \forall v \in V_h, \quad (3.13)$$

$$(\sigma_h, \xi)_Q = 0, \quad \forall \xi \in \mathbb{Q}_h, \quad (3.14)$$

$$(K^{-1} z_h, \zeta)_Q - (p_h, \operatorname{div} \zeta) = 0, \quad \forall \zeta \in Z_h, \quad (3.15)$$

$$c_0 (\partial_t p_h, w) + \alpha (\partial_t A(\sigma_h + \alpha p_h I), wI)_Q + (\operatorname{div} z_h, w) = (q, w), \quad \forall w \in W_h. \quad (3.16)$$

Remark 3.1. We note that the quadrature rule is employed for both $(A(\sigma_h + \alpha p_h I), \tau)_Q$ in (3.12) and $\alpha (\partial_t A(\sigma_h + \alpha p_h I), wI)_Q$ in (3.16), since these two terms will be combined to obtain a coercive term in the well-posedness analysis, while only quadrature rule on the stress term $(A\sigma_h, \tau)_Q$ in (3.12) is needed for local stress elimination.

In the next sections we proceed with establishing existence, uniqueness, stability, and error analysis for the semidiscrete MSMFE-MFMFE method (3.12)–(3.16). In Section 7 we present the fully-discrete MSMFE-MFMFE method and discuss the reduction of the algebraic system at each time step to a symmetric and positive definite cell-centered displacement-pressure system.

4 Existence and uniqueness for the semidiscrete MSMFE-MFMFE method

We first state the inf-sup stability of the mixed Darcy and elasticity spaces, which will be utilized in the analysis. It is known [11] that the spaces $Z_h \times W_h$ satisfy the inf-sup condition

$$\exists \beta_1 > 0 \text{ such that } \forall w_h \in W_h, \quad \sup_{0 \neq \zeta \in Z_h} \frac{(w_h, \operatorname{div} \zeta)}{\|\zeta\|_{\operatorname{div}}} \geq \beta_1 \|w_h\|. \quad (4.1)$$

The inf-sup stability for the mixed elasticity spaces $\mathbb{X}_h \times V_h \times \mathbb{Q}_h$ with quadrature has been studied in [3] on simplices and in [4] on quadrilaterals. In the case of quadrilaterals, the following assumptions on the grid is needed [4]:

- (M1) Each element E has at most one edge on Γ_N^{stress} ,
- (M2) The mesh size h is sufficiently small and there exists a constant C such that for every pair of neighboring elements E and \tilde{E} such that E or \tilde{E} is a non-parallelogram, and every pair of edges $e \subset \partial E \setminus \partial \tilde{E}$, $\tilde{e} \subset \partial \tilde{E} \setminus \partial E$ that share a vertex,

$$|\mathbf{r}_e - \mathbf{r}_{\tilde{e}}|_{\mathbb{R}^2} \leq Ch^2,$$

where \mathbf{r}_e and $\mathbf{r}_{\tilde{e}}$ are the vectors corresponding to e and \tilde{e} , respectively.

We note that (M2) can be thought of as a smoothness assumption on the grid and it is not needed if the grid consists entirely of parallelograms. For the rest of the paper we will tacitly assume that (M1)–(M2) hold on quadrilaterals.

We have the following inf-sup condition on simplices [3] and quadrilaterals [4]:

$$\exists \beta_2 > 0 \text{ such that } \forall v_h \in V_h, \xi_h \in \mathbb{Q}_h, \quad \sup_{0 \neq \tau \in \mathbb{X}_h} \frac{(v_h, \operatorname{div} \tau) + (\xi_h, \tau)_Q}{\|\tau\|_{\operatorname{div}}} \geq \beta_2(\|v_h\| + \|\xi_h\|). \quad (4.2)$$

We note that the semidiscrete method (3.12)–(3.16) is a system of differential-algebraic equations and the standard theory for ordinary differential equations cannot be directly applied. Instead, the well posedness analysis of (3.12)–(3.16) will be based on the existence theory for degenerate parabolic systems, in particular [37, Theorem 6.1(b)].

Theorem 4.1. *Let the linear, symmetric and monotone operator \mathcal{N} be given for the real vector space E to its algebraic dual E^* , and let E'_b be the Hilbert space which is the dual of E with the seminorm*

$$|x|_b = (\mathcal{N}x(x))^{1/2}, \quad x \in E.$$

Let $\mathcal{M} \subset E \times E'_b$ be a relation with domain $D = \{x \in E : \mathcal{M}(x) \neq \emptyset\}$. Assume \mathcal{M} is monotone and $Rg(\mathcal{N} + \mathcal{M}) = E'_b$. Then, for each $x_0 \in D$ and for each $\mathcal{F} \in W^{1,1}(0, T; E'_b)$, there is a solution x of

$$\frac{d}{dt}(\mathcal{N}x(t)) + \mathcal{M}(x(t)) \ni \mathcal{F}(t), \quad 0 < t < T, \quad (4.3)$$

with

$$\mathcal{N}x \in W^{1,\infty}(0, T; E'_b), \quad x(t) \in D, \quad \text{for all } 0 \leq t \leq T, \quad \text{and } \mathcal{N}x(0) = \mathcal{N}x_0.$$

Lemma 4.1. *The semidiscrete MSMFE-MFMFE method (3.12)–(3.16) has a unique solution.*

Proof. In order to fit (3.12)–(3.16) in the form of Theorem 4.1, we consider a slightly modified formulation, with (3.12) differentiated in time and the new variables \dot{u}_h and $\dot{\gamma}_h$ representing $d_t u_h$ and $d_t \gamma_h$, respectively. Introduce the operators

$$\begin{aligned} (A_{\sigma\sigma}\sigma_h, \tau) &= (A\sigma_h, \tau)_Q, \quad (A_{\sigma u}\sigma_h, v) = (\operatorname{div} \sigma_h, v), \quad (A_{\sigma\gamma}\sigma_h, \xi) = (\sigma_h, \xi)_Q, \\ (A_{zz}\zeta_h, \zeta) &= (K^{-1}z_h, \zeta)_Q, \quad (A_{zp}\zeta_h, w) = -(\operatorname{div} z_h, w), \quad (A_{pp}p_h, w) = c_0(p_h, w) + \alpha(A\alpha p_h I, wI)_Q, \end{aligned}$$

we have a system in the form of (4.3), where

$$x = \begin{pmatrix} \sigma_h \\ \dot{u}_h \\ \dot{\gamma}_h \\ z_h \\ p_h \end{pmatrix}, \quad \mathcal{N} = \begin{pmatrix} A_{\sigma\sigma} & 0 & 0 & 0 & A_{\sigma p}^T \\ 0 & 0 & 0 & 0 & 0 \\ 0 & 0 & 0 & 0 & 0 \\ 0 & 0 & 0 & 0 & 0 \\ A_{\sigma p} & 0 & 0 & 0 & A_{pp} \end{pmatrix}, \quad \mathcal{M} = \begin{pmatrix} 0 & A_{\sigma u}^T & A_{\sigma\gamma}^T & 0 & 0 \\ -A_{\sigma u} & 0 & 0 & 0 & 0 \\ -A_{\sigma\gamma} & 0 & 0 & 0 & 0 \\ 0 & 0 & 0 & A_{zz} & A_{zp}^T \\ 0 & 0 & 0 & -A_{zp} & 0 \end{pmatrix}, \quad \mathcal{F} = \begin{pmatrix} 0 \\ -f \\ 0 \\ 0 \\ q \end{pmatrix}.$$

TODO:NEEDS TO BE FINISHED

In the proof of the range condition refer to the proof in [24]. proof is similar using coercivity of quadrature forms.

Need to show that the initial condition is in the domain of the operator. Assume that the true initial condition for all variables is in the domain (see the nonlinear paper) and take the discrete condition to be its elliptic projection.

Note: the stability proof uses initial data for variables other than p and σ .

Need to go back and show existence for our (non-differentiated) method.

NOTE: The error analysis needs to be modified to use the correct initial condition.

□

5 Stability analysis of the semidiscrete MSMFE-MFMFE method

In this section we derive a stability bound for the MSMFE-MFMFE method (3.12)–(3.16). We remark that stability analysis for the \mathcal{BDM}_1 MFE method (3.6)–(3.10) was not performed in [24], where only error analysis was carried out. The stability analysis is more difficult than the error analysis, since

controlling the boundary condition term $\langle g_p, \zeta \cdot n \rangle_{\Gamma_D^{pres}}$ requires bounding $\|\operatorname{div} z_h\|$. Even though we consider $g_p = 0$, we derive a bound on $\|\operatorname{div} z_h\|$, thus obtaining full control on $\|z_h\|_{\operatorname{div}}$.

Step 1: $L^2(\Omega)$ estimates.

We differentiate (3.12) in time, choose $(\tau, v, \xi, \zeta, w) = (\sigma_h, \partial_t u_h, \partial_t \gamma_h, z_h, p_h)$ in equations (3.12)–(3.16), and combine them to obtain

$$(\partial_t(A\sigma_h + \alpha p_h I), \sigma_h + \alpha p_h I)_Q + c_0(\partial_t p_h, p_h) + (K^{-1} z_h, z_h)_Q = (f, \partial_t u_h) + (q, p_h),$$

implying

$$\frac{1}{2} \partial_t \left[\|A^{1/2}(\sigma_h + \alpha p_h I)\|_Q^2 + c_0 \|p_h\|^2 \right] + \|K^{-1/2} z_h\|_Q^2 = (f, \partial_t u_h) + (q, p_h). \quad (5.1)$$

Next, integrating (5.1) in time from 0 to an arbitrary $t \in (0, T]$ results in

$$\begin{aligned} & \frac{1}{2} \left[\|A^{1/2}(\sigma_h + \alpha p_h I)(t)\|_Q^2 + c_0 \|p_h(t)\|^2 \right] + \int_0^t \|K^{-1/2} z_h\|_Q^2 ds \\ &= \int_0^t ((q, p_h) - (\partial_t f, u_h)) ds + \frac{1}{2} \left[\|A^{1/2}(\sigma_h + \alpha p_h I)(0)\|_Q^2 + c_0 \|p_h(0)\|^2 \right] + (f, u_h)(t) + (f, u_h)(0), \end{aligned}$$

Applying the Cauchy-Schwartz and Young's inequalities, we obtain

$$\begin{aligned} & \|A^{1/2}(\sigma_h + \alpha p_h I)(t)\|_Q^2 + c_0 \|p_h(t)\|^2 + 2 \int_0^t \|K^{-1/2} z_h(s)\|_Q^2 ds \\ & \leq \epsilon \left(\|u_h(t)\|^2 + \int_0^t (\|p_h\|^2 + \|u_h\|^2) ds \right) + \frac{1}{\epsilon} \left(\|f(t)\|^2 + \int_0^t (\|q\|^2 + \|\partial_t f\|^2) ds \right) \\ & \quad + \|A^{1/2}(\sigma_h + \alpha p_h I)(0)\|_Q^2 + c_0 \|p_h(0)\|^2 + \|u_h(0)\|^2 + \|f(0)\|^2. \end{aligned} \quad (5.2)$$

TODO: CLEAN UP FROM HERE ON (including deleting all Dirichlet BC terms).

Using the inf-sup condition as in [3, 4] and (3.12), we obtain

$$\begin{aligned} \|u_h\| + \|\gamma_h\| & \leq C \sup_{0 \neq \tau \in \mathbb{X}_h} \frac{(u_h, \operatorname{div} \tau) + (\gamma_h, \tau)_Q}{\|\tau\|_{\operatorname{div}}} \\ & = C \sup_{0 \neq \tau \in \mathbb{X}_h} \frac{-(A^{1/2}(\sigma_h + \alpha p_h I), A^{1/2} \tau)_Q + \langle \mathcal{P}_0 g_u, \tau n \rangle}{\|\tau\|_{\operatorname{div}}} \\ & \leq C \|A^{1/2}(\sigma_h + \alpha p_h I)\| + \|\mathcal{P}_0 g_u\|_{\frac{1}{2}}, \end{aligned} \quad (5.3)$$

where in the last step we used equivalence of norms as stated in Corollary 3.1.

Similarly, using the inf-sup condition [11] and (3.15), we have

$$\begin{aligned} \|p_h\| & \leq C \sup_{0 \neq q \in Z_h} \frac{(p_h, \operatorname{div} q)}{\|q\|_{\operatorname{div}}} = C \sup_{0 \neq q \in Z_h} \frac{(K^{-1} z_h, q)_Q + \langle \mathcal{P}_0 g_p, q \cdot n \rangle}{\|q\|_{\operatorname{div}}} \\ & \leq C \|K^{-1/2} z_h\| + \|\mathcal{P}_0 g_p\|_{\frac{1}{2}}. \end{aligned} \quad (5.4)$$

Combining (5.2)–(5.4), from equivalence of norms we have

$$\begin{aligned} & \|A^{1/2}(\sigma_h(t) + \alpha p_h I(t))\|^2 + \|u_h(t)\|^2 + \|\gamma_h(t)\|^2 + c_0 \|p_h(t)\|^2 + \int_0^t (\|K^{-1/2} z_h(s)\|^2 + \|p_h(s)\|^2) ds \\ & \leq C \left[\epsilon \left(\|u_h(t)\|^2 + \int_0^t (\|p_h(s)\|^2 + \|u_h(s)\|^2) ds \right) + \tilde{\epsilon} \int_0^t (\|\sigma_h(s) n\|_{-1/2} + \|z_h(s) \cdot n\|_{-1/2}) ds \right. \\ & \quad + \frac{C}{\epsilon} \left(\|f(t)\|^2 + \int_0^t (\|g(s)\|^2 + \|\partial_t f(s)\|^2) ds \right) + \frac{C}{\tilde{\epsilon}} \int_0^t (\|\partial_t \mathcal{P}_0 g_u(s)\|_{1/2}^2 + \|\mathcal{P}_0 g_p(s)\|_{1/2}^2) ds \\ & \quad \left. + C \left[\|A^{1/2}(\sigma_h(0) + \alpha p_h I(0))\|_Q^2 + c_0 \|p_h(0)\|^2 + \|u_h(0)\|^2 + \|f(0)\|^2 \right] + \|\mathcal{P}_0 g_u(t)\|_{1/2}^2 \right]. \end{aligned}$$

Finally, choosing ϵ small enough, we obtain the following inequality

$$\begin{aligned}
& \|A^{1/2}(\sigma_h(t) + \alpha p_h I(t))\|^2 + \|u_h(t)\|^2 + \|\gamma_h(t)\|^2 + c_0 \|p_h(t)\|^2 + \int_0^t (\|K^{-1/2} z_h(s)\|^2 + \|p_h(s)\|^2) ds \\
& \leq C \left[\epsilon \int_0^t \|u_h(s)\|^2 ds + \tilde{\epsilon} \int_0^t (\|\sigma_h(s) n\|_{-1/2}^2 + \|z_h(s) \cdot n\|_{-1/2}^2) ds \right. \\
& \quad + \frac{C}{\tilde{\epsilon}} \int_0^t (\|\partial_t \mathcal{P}_0 g_u(s)\|_{1/2}^2 + \|\mathcal{P}_0 g_p(s)\|_{1/2}^2) ds + \left(\|f(t)\|^2 + \int_0^t (\|g(s)\|^2 + \|\partial_t f(s)\|^2) ds \right) \\
& \quad \left. + \|\mathcal{P}_0 g_u(t)\|_{1/2}^2 + \|A^{1/2}(\sigma_h(0) + \alpha p_h I(0))\|_Q^2 + c_0 \|p_h(0)\|^2 + \|u_h(0)\|^2 + \|f(0)\|^2 \right]. \quad (5.5)
\end{aligned}$$

Let us denote the right hand side of (5.5) by H_1 . We proceed with deriving estimates for $\operatorname{div} \sigma_h$ and $\operatorname{div} z_h$.

Step 2: $H(\operatorname{div})$ in space estimate for the stress:

Testing (3.13) with $v = \operatorname{div} \sigma_h$, we immediately obtain a bound on divergence of stress:

$$\|\operatorname{div} \sigma_h\| \leq \|f\|. \quad (5.6)$$

On the other hand setting $\tau = s_h$, $v = u_h$, $\xi = g_h$ in (3.12)-(3.14) and using equivalence of norms, we obtain

$$\|\sigma_h\|^2 \leq C(\|p\|^2 + \|\mathcal{P}_0 g_u\|_{1/2}^2 + \|f\|^2) + \epsilon(\|\sigma_h n\|_{-1/2}^2 + \|u\|^2) \quad (5.7)$$

We combine (5.6)-(5.7) and integrate in time:

$$\begin{aligned}
& \int_0^t (\|\sigma_h(s)\|^2 + \|\operatorname{div} \sigma_h(s)\|^2) ds \\
& \leq C \int_0^t \left((\|p(s)\|^2 + \|\mathcal{P}_0 g_u(s)\|_{1/2}^2 + \|f(s)\|^2) + \epsilon(\|\sigma_h(s) n\|_{-1/2}^2 + \|u(s)\|^2) \right) ds
\end{aligned}$$

Using (5.3), we obtain

$$\begin{aligned}
& \int_0^t (\|\sigma_h(s)\|_{\operatorname{div}}^2 + \|u_h(s)\|^2 + \|\gamma_h(s)\|^2) ds \leq C \int_0^t (\|p(s)\|^2 + \|\mathcal{P}_0 g_u(s)\|_{1/2}^2 + \|f(s)\|^2) ds \\
& \leq H_1 + \int_0^t (\|\mathcal{P}_0 g_u(s)\|_{1/2}^2 + \|f(s)\|^2) ds \quad (5.8)
\end{aligned}$$

Step 3: $H(\operatorname{div})$ in space estimate for the velocity:

It follows from equation (3.16) and Corollary 3.1 that

$$\|\operatorname{div} z_h\| \leq C \left(c_0 \|\partial_t p_h\| + \|A^{1/2} \partial_t (\sigma_h + \alpha p_h I)\| + \|g\| \right). \quad (5.9)$$

To control the first two terms on the right hand side of (5.9), we differentiate equations (3.12)-(3.15) and combine (3.12)-(3.16) as it was done in (??)-(5.2), with the choice $(\tau, v, \xi, q, w) = (\partial_t \sigma_h, \partial_t u_h, \partial_t \gamma_h, z_h, \partial_t p_h)$:

$$\begin{aligned}
& \int_0^t \left(\|A^{1/2} \partial_t (\sigma_h(s) + \alpha p_h I(s))\|_Q^2 + c_0 \|\partial_t p_h(s)\|^2 \right) ds + \frac{1}{2} \|K^{-1/2} z_h(t)\|_Q^2 \\
& \leq \int_0^t (\|p_h(s)\| \|\partial_t g(s)\| + \|\partial_t u_h(s)\| \|\partial_t f(s)\| + \|\sigma_h n\|_{-1/2} \|\partial_t \mathcal{P}_0 g_u\|_{1/2} + \|z_h \cdot n\|_{-1/2} \|\partial_t \mathcal{P}_0 g_p\|_{1/2}) ds \\
& \quad + \|p_h(t)\| \|g(t)\| + \frac{1}{2} \|K^{-1/2} z_h(0)\|_Q^2 - \|p_h(0)\| \|g(0)\|. \quad (5.10)
\end{aligned}$$

Using the inf-sup condition [3, 4] and (3.12), differentiated in time, we get

$$\|\partial_t u_h\| + \|\partial_t \gamma_h\| \leq C \|A^{1/2} \partial_t (\sigma_h + \alpha p_h I)\| + \|\partial_t \mathcal{P}_0 g_u\|_{\frac{1}{2}}. \quad (5.11)$$

Combining (5.4), (5.11) and (5.10), we get:

$$\begin{aligned}
& \int_0^t \left(\|A^{1/2} \partial_t(\sigma_h(s) + \alpha p_h I(s))\|^2 + \|\partial_t u_h(s)\|^2 + \|\partial_t \gamma_h(s)\|^2 + c_0 \|\partial_t p_h(s)\|^2 \right) ds \\
& + \|K^{-1/2} z_h(t)\|^2 + \|p_h(t)\|^2 \\
& \leq \epsilon \left(\int_0^t (\|p_h(s)\|^2 + \|\partial_t u_h(s)\|^2) ds + \|p_h(t)\|^2 \right) + \tilde{\epsilon} \int_0^t (\|\sigma_h(s) n\|_{-1/2}^2 + \|z_h(s) \cdot n\|_{-1/2}^2) ds \\
& + \frac{C}{\epsilon} \left(\int_0^t (\|\partial_t g(s)\|^2 + \|\partial_t f(s)\|^2) ds + \|g(t)\|^2 \right) + \frac{C}{\tilde{\epsilon}} \int_0^t (\|\partial_t \mathcal{P}_0 g_u(s)\|_{1/2}^2 + \|\partial_t \mathcal{P}_0 g_p(s)\|_{1/2}^2) ds \\
& + C(\|z_h(0)\|^2 + \|p_h(0)\|^2 + \|g(0)\|^2).
\end{aligned}$$

Choosing ϵ small enough, we obtain

$$\begin{aligned}
& \int_0^t \left(\|A^{1/2} \partial_t(\sigma_h(s) + \alpha p_h I(s))\|^2 + \|\partial_t u_h(s)\|^2 + \|\partial_t \gamma_h(s)\|^2 + c_0 \|\partial_t p_h(s)\|^2 \right) ds \\
& + \|K^{-1/2} z_h(t)\|^2 + \|p_h(t)\|^2 \\
& \leq \tilde{\epsilon} \int_0^t (\|\sigma_h(s) n\|_{-1/2}^2 + \|z_h(s) \cdot n\|_{-1/2}^2) ds + \frac{C}{\tilde{\epsilon}} \int_0^t (\|\partial_t \mathcal{P}_0 g_u(s)\|_{1/2}^2 + \|\partial_t \mathcal{P}_0 g_p(s)\|_{1/2}^2) ds \\
& + C \left(\int_0^t (\|\partial_t g(s)\|^2 + \|\partial_t f(s)\|^2) ds + \|g(t)\|^2 + \|z_h(0)\|^2 + \|p_h(0)\|^2 + \|g(0)\|^2 + H_1 \right). \quad (5.12)
\end{aligned}$$

Integrating (5.9) in time and using (5.12), results in

$$\begin{aligned}
& \int_0^t \|\operatorname{div} z_h(s)\|^2 ds + \|K^{-1/2} z_h(t)\|^2 + \|p_h(t)\|^2 \\
& \leq \tilde{\epsilon} \int_0^t (\|\sigma_h(s) n\|_{-1/2}^2 + \|z_h(s) \cdot n\|_{-1/2}^2) ds + \frac{C}{\tilde{\epsilon}} \int_0^t (\|\partial_t \mathcal{P}_0 g_u(s)\|_{1/2}^2 + \|\partial_t \mathcal{P}_0 g_p(s)\|_{1/2}^2) ds \\
& + C \left(\int_0^t (\|g(s)\|^2 + \|\partial_t g(s)\|^2 + \|\partial_t f(s)\|^2) ds + \|g(t)\|^2 + \|z_h(0)\|^2 + \|p_h(0)\|^2 + \|g(0)\|^2 + H_1 \right). \quad (5.13)
\end{aligned}$$

We note that initial condition for Darcy velocity can be computed as a suitable projection of $-K \nabla p(0)$, provided the initial condition is regular enough.

Step 4: obtaining the final result:

We combine (5.5), (5.8) and (5.13):

$$\begin{aligned}
& \|A^{1/2}(\sigma_h(t) + \alpha p_h I(t))\|^2 + \|u_h(t)\|^2 + \|\gamma_h(t)\|^2 + \|z_h(t)\|^2 + \|p_h(t)\|^2 \\
& + \int_0^t (\|\sigma_h(s)\|_{\operatorname{div}}^2 + \|u_h(s)\|^2 + \|\gamma_h(s)\|^2 + \|z_h(s)\|_{\operatorname{div}}^2 + \|p_h(s)\|^2) ds \\
& \leq C \left[\int_0^t \left(\|\mathcal{P}_0 g_u(s)\|_{1/2} + \|\partial_t \mathcal{P}_0 g_u(s)\|_{1/2} + \|\mathcal{P}_0 g_p(s)\|_{1/2} + \|\partial_t \mathcal{P}_0 g_p(s)\|_{1/2} + \|g(s)\|^2 \right. \right. \\
& \quad \left. \left. + \|\partial_t g(s)\|^2 + \|f(s)\|^2 + \|\partial_t f(s)\|^2 \right) ds + \epsilon \int_0^t \|u_h(s)\|^2 ds + \|f(t)\|^2 + \|g(t)\|^2 + \|\mathcal{P}_0 g_u(t)\|_{1/2} \right. \\
& \quad \left. + \|f(0)\|^2 + \|g(0)\|^2 + \|A^{1/2}(\sigma_h(0) + \alpha p_h I(0))\|_Q^2 + \|p_h(0)\|^2 + \|u_h(0)\|^2 + \|z_h(0)\|^2 \right]. \quad (5.14)
\end{aligned}$$

Note that we can also obtain an estimate on $\|\sigma_h(t)\|$ as follows:

$$\begin{aligned}
\|\sigma_h(t)\| & \leq C \|A^{1/2} \sigma_h(t)\| \leq C \left(\|A^{1/2}(\sigma_h(t) + \alpha p_h I(t))\| + \|A^{1/2} \alpha p_h I(t)\| \right) \\
& \leq C \left(\|A^{1/2}(\sigma_h(t) + \alpha p_h I(t))\| + \|p_h(t)\| \right) \quad (5.15)
\end{aligned}$$

Then, (5.15) together with (5.6) yield

$$\|\sigma_h(t)\|_{\operatorname{div}} \leq C \left(\|A^{1/2}(\sigma_h(t) + \alpha p_h I(t))\| + \|p_h(t)\| + \|f(t)\| \right) \quad (5.16)$$

Finally, (5.14)-(5.16) yield the following result.

Theorem 5.1. *Let $(\sigma_h, u_h, \gamma_h, z_h, p_h) \in \mathbb{X}_h \times V_h \times \Theta_h \times Z_h \times W_h$ be the solution of (3.12)-(3.16). Then the following stability estimate holds:*

$$\begin{aligned}
& \|\sigma_h\|_{L^\infty(0,T;H(\text{div},\Omega))} + \|u_h\|_{L^\infty(0,T;L^2(\Omega))} + \|\gamma_h\|_{L^\infty(0,T;L^2(\Omega))} + \|z_h\|_{L^\infty(0,T;L^2(\Omega))} + \|p_h\|_{L^\infty(0,T;L^2(\Omega))} \\
& + \|\sigma_h\|_{L^2(0,T;H(\text{div},\Omega))} + \|u_h\|_{L^2(0,T;L^2(\Omega))} + \|\gamma_h\|_{L^2(0,T;L^2(\Omega))} + \|z_h\|_{L^2(0,T;H(\text{div},\Omega))} + \|p_h\|_{L^2(0,T;L^2(\Omega))} \\
& \leq C \left[\|p_h(0)\| + \|\sigma_h(0)\| + \|u_h(0)\| + \|z_h(0)\| + \|f\|_{L^\infty(0,T;L^2(\Omega))} + \|f\|_{H^1(0,T;L^2(\Omega))} \right. \\
& + \|g_p\|_{H^1(0,T;H^{1/2}(\partial\Omega))} + \|g\|_{L^\infty(0,T;L^2(\Omega))} + \|g\|_{H^1(0,T;L^2(\Omega))} \\
& \left. + \|g_u\|_{L^\infty(0,T;H^{1/2}(\partial\Omega))} + \|g_u\|_{H^1(0,T;H^{1/2}(\partial\Omega))} \right]. \tag{5.17}
\end{aligned}$$

6 Error analysis

6.1 Preliminaries

Due to the reduced approximation properties of the MFE spaces on general quadrilaterals [6], we restrict the quadrilateral elements to be $O(h^2)$ -perturbations of parallelograms:

$$\|\mathbf{r}_{34} - \mathbf{r}_{21}\| \leq Ch^2.$$

In this case it is easy to verify (see [43] for details) that

$$|DF_E|_{1,\infty,\hat{E}} \leq Ch^2 \quad \text{and} \quad \left| \frac{1}{J_E} DF_E \right|_{j,\infty,\hat{E}} \leq Ch^{j-1}, \quad j = 1, 2. \tag{6.1}$$

We introduce the L^2 -projection operators $Q^0 : L^2(\Omega) \rightarrow W_h$ and $Q^1 : L^2(\Omega) \rightarrow \mathbb{Q}_h$ satisfying

$$(\phi - Q^0 \phi, \psi_h) = 0, \quad \forall \psi_h \in W_h, \tag{6.2}$$

$$(\phi - Q^1 \phi, \psi_h) = 0, \quad \forall \psi_h \in \mathbb{Q}_h. \tag{6.3}$$

We will use projection operator Q^1 for approximation of the rotation variable, and Q^0 operator for approximation of the pressure. Notice also, that the same operator Q^0 applied component-wise can be used for approximation of the displacement variable.

We denote by Π a mixed projection operator acting on tensor valued functions, such that $\Pi : \mathbb{X} \cap H^1(\Omega, \mathbb{M}) \rightarrow \mathbb{X}_h$. We will also use the same notation for a projection operator acting on vector valued functions, so that in this case Π maps from $Z \cap H^1(\Omega, \mathbb{R}^d)$ onto Z_h . It was shown in [10, 11] and [38] that such projection operator exists and satisfies the following properties

$$\begin{aligned}
(\text{div}(\Pi\tau - \tau), v) &= 0, & \forall v \in V_h, \\
(\text{div}(\Pi\zeta - \zeta), w) &= 0, & \forall w \in W_h.
\end{aligned} \tag{6.4}$$

We will also make use of the mixed projection operator onto the lowest order Raviart-Thomas space \mathcal{RT}_0 [33, 11]. This additional construction is needed only for the error analysis on quadrilaterals, although for uniformity in the forthcoming proofs we will treat the simplicial case in the same fashion. We denote the \mathcal{RT}_0 -based spaces by \mathbb{X}_h^0 and Z_h^0 for tensors and vectors, respectively, where the former is obtained from d copies of the latter. The degrees of freedom of \mathbb{X}_h^0 or Z_h^0 are constant values of the normal stress or velocity on all edges (faces). The \mathcal{RT}_0 mixed projection operator, denoted by Π^0 , has properties similar to the \mathcal{BDM}_1 projection operator Π . It also satisfies

$$\begin{aligned}
\text{div} \Pi_0 \tau &= \text{div} \tau \quad \text{and} \quad \|\Pi_0 \tau\| \leq C \|\tau\| \quad \forall \tau \in \mathbb{X}_h, \\
\text{div} \Pi_0 \zeta &= \text{div} \zeta \quad \text{and} \quad \|\Pi_0 \zeta\| \leq C \|\zeta\| \quad \forall \zeta \in Z_h.
\end{aligned} \tag{6.5}$$

The following lemma summarizes well-known continuity and approximation properties of the projection operators, where $\mathbb{H} \in \{\mathbb{M}, \mathbb{R}^d\}$.

Lemma 6.1. *There exists a constant $C > 0$ such that*

$$\|\phi - Q^0\phi\| \leq C\|\phi\|_r h^r, \quad \forall \phi \in H^r(\Omega), \quad 0 \leq r \leq 1, \quad (6.6)$$

$$\|\phi - Q^1\phi\| \leq C\|\phi\|_r h^r, \quad \forall \phi \in H^r(\Omega), \quad 0 \leq r \leq 1, \quad (6.7)$$

$$\|\psi - \Pi\psi\| \leq C\|\psi\|_r h^r, \quad \forall \psi \in H^r(\Omega, \mathbb{H}), \quad 1 \leq r \leq 2, \quad (6.8)$$

$$\|\psi - \Pi^0\psi\| \leq C\|\psi\|_1 h, \quad \forall \psi \in H^1(\Omega, \mathbb{H}), \quad (6.9)$$

$$\|\operatorname{div}(\psi - \Pi\psi)\| + \|\operatorname{div}(\psi - \Pi^0\psi)\| \leq C\|\operatorname{div}\psi\|_r h^r, \quad \forall \psi \in H^{r+1}(\Omega, \mathbb{H}), \quad 0 \leq r \leq 1. \quad (6.10)$$

In addition, for all elements $E \in \mathcal{T}_h$, there exists a constant $C > 0$, such that

$$\|\Pi\psi\|_{1,E} \leq C\|\psi\|_{1,E}, \quad \forall \psi \in H^1(E, \mathbb{H}), \quad (6.11)$$

$$\|Q^1\phi\|_{1,E} \leq C\|\phi\|_{1,E}, \quad \forall \phi \in H^1(E), \quad (6.12)$$

Proof. The proof of bounds for the L^2 -projections (6.6)-(6.7) can be found in [13]; and bounds (6.8)-(6.10) can be found in [11, 34] for affine elements and [38, 6] for h^2 -parallelograms. Finally, the proof of (6.11)-(6.12) was presented in [43]. \square

The following result is needed in the error analysis.

Lemma 6.2. *For any $\hat{\chi} \in \hat{\mathbb{X}}_h(\hat{E})$ and $\hat{r} \in \hat{Z}_h(\hat{E})$,*

$$(\hat{\chi} - \hat{\Pi}_0\hat{\chi}, \hat{\tau}_0)_{\hat{Q}, \hat{E}} = 0 \quad \text{for all constant tensors } \hat{\tau}_0, \quad (6.13)$$

$$(\hat{r} - \hat{\Pi}_0\hat{r}, \hat{v}_0)_{\hat{Q}, \hat{E}} = 0 \quad \text{for all constant vectors } \hat{v}_0. \quad (6.14)$$

Proof. The property (6.14) was shown in [43, Lemma 2.2] on the reference square. The proof on the reference simplex follows in a similar way. The property (6.13) follows from (6.14). \square

For $\phi, \psi \in \mathbb{X}_h$ or $\phi, \psi \in Z_h$, $\tau \in \mathbb{X}_h$ and $\zeta \in \mathbb{Q}_h$ or $\zeta \in (W_h)^{d \times d}$ denote the quadrature error by

$$\theta(L\phi, \psi) := (L\phi, \psi) - (L\phi, \psi)_Q. \quad (6.15)$$

The next result summarizes the quadrature error bounds.

Lemma 6.3. *If $K^{-1} \in W_{\mathcal{T}_h}^{1,\infty}$ and $A \in W_{\mathcal{T}_h}^{1,\infty}$, then there is a constant $C > 0$ such that*

$$|\theta(K^{-1}q, v)| \leq C \sum_{E \in \mathcal{T}_h} h \|K^{-1}\|_{1,\infty,E} \|q\|_{1,E} \|v\|_E, \quad \forall q \in V_h, v \in V_h^0, \quad (6.16)$$

$$|\theta(A\tau, \chi + wI)| \leq C \sum_{E \in \mathcal{T}_h} h \|A\|_{1,\infty,E} \|\tau\|_{1,E} \|\chi + wI\|_E, \quad \forall \tau \in \mathbb{X}_h, \chi \in \mathbb{X}_h^0, w \in W_h, \quad (6.17)$$

$$|\theta(AwI, r)| \leq C \sum_{E \in \mathcal{T}_h} h \|A\|_{1,\infty,E} \|w\|_E \|r\|_E, \quad \forall w, r \in W_h, \quad (6.18)$$

$$|\theta(\chi, \xi)| \leq C \sum_{E \in \mathcal{T}_h} h \|\chi\|_{1,E} \|\xi\|_E, \quad \forall \chi \in \mathbb{X}_h^0, \xi \in \Theta_h, \quad (6.19)$$

$$\left| (K^{-1}\Pi u, v - \Pi^0 v)_Q \right| \leq Ch \|K^{-1}\|_{1,\infty,\mathcal{T}_h} \|u\|_1 \|v\|, \quad \forall u \in H^1(\Omega, \mathbb{R}^d), v \in V_h, \quad (6.20)$$

$$\left| (A(\Pi\sigma + Q^0 p), \chi - \Pi^0 \chi)_Q \right| \leq Ch \|A\|_{1,\infty,\mathcal{T}_h} (\|\sigma\|_1 + \|p\|_1) \|\chi\|, \quad \forall \sigma \in H^1(\Omega, \mathbb{M}), p \in H^1(\Omega), \chi \in \mathbb{X}_h, \quad (6.21)$$

$$\left| (\chi - \Pi^0 \chi, Q^1 \gamma)_Q \right| \leq Ch \|\gamma\|_1 \|\chi\|, \quad \forall \gamma \in H^1(\Omega, \mathbb{N}), \chi \in \mathbb{X}_h. \quad (6.22)$$

Proof. The estimates (6.16) and (6.20) can be found in [43]. We note that (6.20) was stated only on quadrilaterals in [43], but it also holds on simplices, since it follows from mapping to the reference element and (6.14). Bounds (6.17)–(6.19) were proven in [3] on simplices and in [4] on quadrilaterals. Bounds (6.21) and (6.22) were shown in [4] on quadrilaterals. Their proof on simplices is similar, using (6.13). \square

6.2 Optimal convergence

We form the error system by subtracting the discrete problem (3.12)-(3.16) from the continuous one (3.6)-(3.10)

$$(A\sigma, \tau) - (A\sigma_h, \tau)_Q + (A\alpha p I, \tau) - (A\alpha p_h I, \tau)_Q + (u - u_h, \operatorname{div} \tau) + (\gamma, \tau) - (\gamma_h, \tau)_Q = \langle g_u - \mathcal{P}_0 g_u, \tau n \rangle, \quad \forall \tau \in \mathbb{X}_h, \quad (6.23)$$

$$(\operatorname{div} \sigma - \operatorname{div} \sigma_h, v) = 0, \quad \forall v \in V_h, \quad (6.24)$$

$$(\sigma, \xi) - (\sigma_h, \xi)_Q = 0, \quad \forall \xi \in \Theta_h, \quad (6.25)$$

$$(K^{-1}z, q) - (K^{-1}z_h, q)_Q - (p - p_h, \operatorname{div} q) = \langle g_p - \mathcal{P}_0 g_p, q \cdot n \rangle, \quad \forall q \in Z_h, \quad (6.26)$$

$$c_0 (\partial_t p - \partial_t p_h, w) + \alpha (\partial_t \operatorname{tr}(A\sigma), w) - \alpha (\partial_t \operatorname{tr}(A\sigma_h), w)_Q + \alpha (\partial_t \operatorname{tr}(A\alpha p I), w) - \alpha (\partial_t \operatorname{tr}(A\alpha p_h I), w)_Q + (\operatorname{div} z - \operatorname{div} z_h, w) = 0, \quad \forall w \in W_h. \quad (6.27)$$

We split the errors into approximation and discrete errors as follows:

$$\begin{aligned} \sigma - \sigma_h &= (\sigma - \Pi\sigma) + (\Pi\sigma - \sigma_h) := \psi_\sigma + \phi_\sigma, \\ u - u_h &= (u - Q^0 u) + (Q^0 u - u_h) := \psi_u + \phi_u, \\ \gamma - \gamma_h &= (\gamma - Q^1 \gamma) + (Q^1 \gamma - \gamma_h) := \psi_\gamma + \phi_\gamma, \\ z - z_h &= (z - \Pi z) + (\Pi z - z_h) := \psi_z + \phi_z, \\ p - p_h &= (p - Q^0 p) + (Q^0 p - p_h) := \psi_p + \phi_p. \end{aligned}$$

Step 1: L^2 in space estimates:

With these notations we can rewrite the first equation (6.23) in the error system in the following way:

$$\begin{aligned} &(A\phi_\sigma, \tau)_Q + \alpha (A\phi_p I, \tau)_Q + (\phi_u, \operatorname{div} \tau) + (\phi_\gamma, \tau)_Q \\ &= (A\Pi\sigma, \tau)_Q - (A\sigma, \tau) + \alpha (AQ^0 p I, \tau)_Q - \alpha (Ap I, \tau) + (\psi_u, \operatorname{div} \tau) \\ &\quad + (Q^1 \gamma, \tau)_Q - (\gamma, \tau) + \langle g_u - \mathcal{P}_0 g_u, \tau n \rangle. \end{aligned}$$

It follows from the definition of Q^0 operator (6.2) that $(\psi_u, \operatorname{div} \tau) = 0$. Combining the rest of the terms, we write

$$\begin{aligned} &(A\phi_\sigma, \tau)_Q + \alpha (A\phi_p I, \tau)_Q + (\phi_u, \operatorname{div} \tau) + (\phi_\gamma, \tau)_Q \\ &= - (A(\sigma + \alpha p I), \tau - \Pi^0 \tau) - (A(\psi_\sigma + \alpha \psi_p I), \Pi^0 \tau) - (A(\Pi\sigma + \alpha Q^0 p I), \Pi^0 \tau) \\ &\quad + (A(\Pi\sigma + \alpha Q^0 p I), \Pi^0 \tau)_Q + (A(\Pi\sigma + \alpha Q^0 p I), \tau - \Pi^0 \tau)_Q - (\gamma, \tau - \Pi^0 \tau) - (\psi_\gamma, \Pi^0 \tau) \\ &\quad - (Q^1 \gamma, \Pi^0 \tau) + (Q^1 \gamma, \Pi^0 \tau)_Q + (Q^1 \gamma, \tau - \Pi^0 \tau)_Q + \langle g_u, (\tau - \Pi^0 \tau) n \rangle, \end{aligned} \quad (6.28)$$

where we also used (??). Taking $\tau - \Pi^0 \tau$ as a test function in (3.6), we obtain

$$(A(\sigma + \alpha p I), \tau - \Pi^0 \tau) + (u, \operatorname{div} (\tau - \Pi^0 \tau)) + (\gamma, \tau - \Pi^0 \tau) = \langle g_u, (\tau - \Pi^0 \tau) n \rangle.$$

Hence, due to (??) and (6.5),

$$- (A(\sigma + \alpha p I), \tau - \Pi^0 \tau) - (\gamma, \tau - \Pi^0 \tau) + \langle g_u, (\tau - \Pi^0 \tau) n \rangle = 0. \quad (6.29)$$

Combining (6.28)-(6.29) and rewriting terms, coming from the use of quadrature rule, we get

$$\begin{aligned} &(A\phi_\sigma, \tau)_Q + \alpha (A\phi_p I, \tau)_Q + (\phi_u, \operatorname{div} \tau) + (\phi_\gamma, \tau)_Q \\ &= - (A(\psi_\sigma + \alpha \psi_p I), \Pi^0 \tau) - (\psi_\gamma, \Pi^0 \tau) - \theta (A\Pi\sigma, \Pi^0 \tau) - \theta (A\alpha Q^0 p I, \Pi^0 \tau) \\ &\quad - \theta (Q^1 \gamma, \Pi^0 \tau) + (A(\Pi\sigma + \alpha Q^0 p I), \tau - \Pi^0 \tau)_Q + (Q^1 \gamma, \tau - \Pi^0 \tau)_Q. \end{aligned} \quad (6.30)$$

From (6.4) and (6.24) we have

$$\operatorname{div} \phi_\sigma = 0. \quad (6.31)$$

We rewrite (6.26) similarly to how it was done in (6.28)-(6.30):

$$\begin{aligned} (K^{-1}\phi_z, q)_q - (\phi_p, \operatorname{div} q) &= (\psi_p, \operatorname{div} q) - (K^{-1}z, q - \Pi^0 q) - (K^{-1}(z - \Pi z), \Pi^0 q) - (K^{-1}\Pi z, \Pi^0 q) \\ &\quad + (K^{-1}\Pi z, \Pi_0 q)_Q + (K^{-1}\Pi z, q - \Pi^0 q)_Q - \langle g_p, (q - \Pi^0 q) \cdot n \rangle. \end{aligned}$$

Using (6.2), we conclude that $(\psi_p, \operatorname{div} q) = 0$. Moreover, testing (3.6) with $q - \Pi^0 q$, we also obtain

$$- (K^{-1}z, q - \Pi^0 q) - \langle g_p, (q - \Pi^0 q) \cdot n \rangle = 0.$$

Hence, we have

$$(K^{-1}\phi_z, q)_Q - (\phi_p, \operatorname{div} q) = - (K^{-1}\psi_z, \Pi^0 q) - \theta (K^{-1}\Pi z, \Pi^0 q) + (K^{-1}\Pi z, q - \Pi^0 q)_Q. \quad (6.32)$$

Finally, using (6.2) and (??), we rewrite the last equation, (6.27), in the error system as follows

$$\begin{aligned} c_0 (\partial_t \phi_p, w) + \alpha (\partial_t \operatorname{tr}(A\phi_\sigma), w)_Q + \alpha^2 (\partial_t \operatorname{tr}(A\phi_p), w)_Q + (\operatorname{div} \phi_z, w) - \alpha (\partial_t \operatorname{tr}(A\psi_\sigma), w) \\ = -\alpha\theta (\partial_t \operatorname{tr}(A\Pi\sigma), w) - \alpha^2 (\partial_t \operatorname{tr}(A\psi_p I), w) - \alpha^2 \theta (\partial_t \operatorname{tr}(AQ^0 p I), w). \end{aligned} \quad (6.33)$$

Next we differentiate (6.30), set $\tau = \phi_\sigma$, $\xi = \partial_t \phi_\gamma$, $q = \phi_z$, $w = \phi_p$ and combine (6.30)-(6.32):

$$\begin{aligned} \frac{1}{2} \partial_t \left[\|A^{1/2}(\phi_\sigma + \alpha\phi_p I)\|_Q^2 + c_0 \|\phi_p\|^2 \right] + (K^{-1}\phi_z, \phi_z)_Q \\ = - (A\partial_t(\psi_\sigma + \alpha\psi_p I), \Pi^0 \phi_\sigma) - (\partial_t \psi_\gamma, \Pi^0 \phi_\sigma) - \theta (A\partial_t \Pi\sigma, \Pi^0 \phi_\sigma + \alpha\phi_p I) \\ - \theta (\partial_t Q^1 \gamma, \Pi^0 \phi_\sigma) + (A\partial_t(\Pi\sigma + \alpha Q^0 p I), \phi_\sigma - \Pi^0 \phi_\sigma)_Q + (\partial_t Q^1 \gamma, \phi_\sigma - \Pi^0 \phi_\sigma)_Q \\ - (K^{-1}\psi_z, \Pi^0 \phi_z) - \theta (K^{-1}\Pi z, \Pi^0 \phi_z) + (K^{-1}\Pi z, \phi_z - \Pi^0 \phi_z)_Q - \alpha (\partial_t \operatorname{tr}(A\psi_\sigma), \phi_p) \\ - \alpha^2 (\partial_t \operatorname{tr}(A\psi_p I), \phi_p) - \alpha\theta (\partial_t AQ^0 p I, \Pi^0 \phi_\sigma + \alpha\phi_p). \end{aligned} \quad (6.34)$$

Using (6.6)-(6.8) and (6.5), we have

$$\begin{aligned} \left| (A\partial_t(\psi_\sigma + \alpha\psi_p I), \Pi^0 \phi_\sigma) + (\partial_t \psi_\gamma, \Pi^0 \phi_\sigma) + (K^{-1}\psi_z, \Pi^0 \phi_z) \right. \\ \left. + \alpha (\partial_t \operatorname{tr}(A\psi_\sigma), \phi_p) - \alpha^2 (\partial_t \operatorname{tr}(A\psi_p I), \phi_p)_Q \right| \\ \leq Ch^2(\|\partial_t \sigma\|_1^2 + \|\partial_t p\|_1^2 + \|\partial_t \gamma\|_1^2 + \|z\|_1^2) + \epsilon(\|\phi_\sigma\|^2 + \|\phi_p\|^2 + \|\phi_z\|^2). \end{aligned} \quad (6.35)$$

Applying (6.16)-(6.19) and continuity of projection operators

$$\begin{aligned} \left| \theta (A\partial_t \Pi\sigma, \Pi^0 \phi_\sigma + \alpha\phi_p I) + \theta (K^{-1}\Pi z, \Pi^0 \phi_z) - \alpha\theta (\partial_t AQ^0 p I, \Pi^0 \phi_\sigma + \alpha\phi_p) - \theta (\partial_t Q^1 \gamma, \Pi^0 \phi_\sigma) \right| \\ \leq Ch^2(\|\partial_t \sigma\|_1^2 + \|z\|_1^2 + \|\partial_t p\|_0^2 + \|\partial_t \gamma\|_0^2) + \epsilon(\|\phi_\sigma\|^2 + \|\phi_p\|^2 + \|\phi_z\|^2). \end{aligned} \quad (6.36)$$

Due to (6.20) -(6.22) ,

$$\begin{aligned} \left| (A\partial_t(\Pi\sigma + \alpha Q^0 p I), \phi_\sigma - \Pi^0 \phi_\sigma)_Q + (\partial_t Q\gamma, \phi_\sigma - \Pi^0 \phi_\sigma)_Q + (K^{-1}\Pi z, \phi_z - \Pi^0 \phi_z)_Q \right| \\ \leq Ch^2(\|\partial_t \sigma\|_1^2 + \|\partial_t p\|_1^2 + \|\partial_t \gamma\|_1^2 + \|z\|_1^2) + \epsilon(\|\phi_\sigma\|^2 + \|\phi_z\|^2). \end{aligned} \quad (6.37)$$

Next, we combine (6.34)-(6.37) and integrate the result in time from 0 to arbitrary $t \in (0, T]$:

$$\begin{aligned} \|A^{1/2}(\phi_\sigma(t) + \alpha\phi_p I(t))\|_Q^2 + c_0 \|\phi_p(t)\|^2 + \int_0^t \|K^{-1/2}\phi_z(s)\|_Q^2 ds \\ \leq \epsilon \int_0^t (\|\phi_\sigma(s)\|^2 + \|\phi_p(s)\|^2 + \|\phi_z(s)\|^2) ds \\ + Ch^2 \int_0^t (\|\partial_t \sigma(s)\|_1^2 + \|\partial_t p(s)\|_1^2 + \|\partial_t \gamma(s)\|_1^2 + \|z(s)\|_1^2) ds \\ + \|A^{1/2}(\phi_\sigma(0) + \alpha\phi_p I(0))\|_Q^2 + c_0 \|\phi_p(0)\|^2. \end{aligned} \quad (6.38)$$

Choosing $\sigma_h(0) = \Pi\sigma(0)$ and $p_h(0) = Q^0p(0)$, we obtain

$$\|A^{1/2}(\phi_\sigma(0) + \alpha\phi_p I(0))\|_Q^2 + c_0\|\phi_p(0)\|^2 = 0. \quad (6.39)$$

Hence, we can write (6.38) as

$$\begin{aligned} & \|A^{1/2}(\phi_\sigma(t) + \alpha\phi_p I(t))\|_Q^2 + c_0\|\phi_p(t)\|^2 + \int_0^t \|K^{-1/2}\phi_z(s)\|_Q^2 ds \\ & \leq \epsilon \int_0^t (\|\phi_\sigma(s)\|^2 + \|\phi_p(s)\|^2 + \|\phi_z(s)\|^2) ds \\ & \quad + Ch^2 \int_0^t (\|\partial_t \sigma(s)\|_1^2 + \|\partial_t p(s)\|_1^2 + \|\partial_t \gamma(s)\|_1^2 + \|z(s)\|_1^2) ds. \end{aligned} \quad (6.40)$$

Using the inf-sup condition [3, 4] and (6.23), we get

$$\begin{aligned} \|\phi_u\| + \|\phi_\gamma\| & \leq C \sup_{0 \neq \tau \in \mathbb{X}_h} \frac{(\phi_u, \operatorname{div} \tau) + (\phi_\gamma, \tau)_Q}{\|\tau\|_{\operatorname{div}}} \\ & = C \sup_{0 \neq \tau \in \mathbb{X}_h} \left(\frac{(A(\sigma_h + \alpha p_h I), \tau)_Q - (A(\sigma + \alpha p I), \tau)}{\|\tau\|_{\operatorname{div}}} \right. \\ & \quad \left. + \frac{(Q^1 \gamma, \tau) - (\gamma, \tau)_Q + \langle g_u - Q^0 g_u, \tau n \rangle}{\|\tau\|_{\operatorname{div}}} \right). \end{aligned} \quad (6.41)$$

Using the calculations as in (6.28)-(6.30), (??) and (??), we have

$$\begin{aligned} & (A(\sigma_h + \alpha p_h I), \tau)_Q - (A(\sigma + \alpha p I), \tau) + (Q^1 \gamma, \tau) - (\gamma, \tau)_Q + \langle g_u - \mathcal{P}_0 g_u, \tau n \rangle \\ & = - (A(\phi_\sigma + \alpha \phi_p I), \tau)_Q - (A(\psi_\sigma + \alpha \psi_p I), \Pi^0 \tau) - (\psi_\gamma, \Pi^0 \tau) - \theta (A \Pi \sigma, \Pi^0 \tau) \\ & \quad + (A(\Pi \sigma + \alpha Q^0 p I), \tau - \Pi^0 \tau)_Q + (Q^1 \gamma, \tau - \Pi^0 \tau)_Q \\ & \leq Ch(\|\sigma\|_1 + \|p\|_1 + \|\gamma\|_1)\|\tau\| + C\|A^{1/2}(\phi_\sigma + \alpha \phi_p I)\|\|\tau\| \end{aligned} \quad (6.42)$$

Combining (6.41) and (6.42) and using orthogonality of projections, we get

$$\|\phi_u\| + \|\phi_\gamma\| \leq Ch(\|\sigma\|_1 + \|p\|_1 + \|\gamma\|_1) + C\|A^{1/2}(\phi_\sigma + \alpha \phi_p I)\|.$$

Thus, (6.40) becomes

$$\begin{aligned} & \|A^{1/2}(\phi_\sigma(t) + \alpha\phi_p I(t))\|^2 + \|\phi_u(t)\|^2 + \|\phi_\gamma(t)\|^2 + c_0\|\phi_p(t)\|^2 + \int_0^t \|\phi_z(s)\|^2 ds \\ & \leq \epsilon \int_0^t (\|\phi_\sigma(s)\|^2 + \|\phi_p(s)\|^2 + \|\phi_z(s)\|^2) ds + Ch^2(\|\sigma(t)\|_1^2 + \|p(t)\|_1^2 + \|\gamma(t)\|_1^2), \\ & \quad + Ch^2 \int_0^t (\|\partial_t \sigma(s)\|_1^2 + \|\partial_t p(s)\|_1^2 + \|\partial_t \gamma(s)\|_1^2 + \|z(s)\|_1^2) ds, \end{aligned} \quad (6.43)$$

where we also used the equivalence of norms, see Corollary 3.1.

Using the fact that $Z_h^0 \times W_h$ is a stable Darcy pair, (6.26), (??), (6.8) and (6.16) we also obtain

$$\begin{aligned} \|\phi_p\| & \leq C \sup_{0 \neq q \in Z_h^0} \frac{(\operatorname{div} q, \phi_p)}{\|q\|_{\operatorname{div}}} = C \sup_{0 \neq q \in Z_h^0} \frac{(K^{-1}z, q) - (K^{-1}z_h, q)_Q}{\|q\|_{\operatorname{div}}} \\ & = C \sup_{0 \neq q \in Z_h^0} \frac{(K^{-1}\phi_z, q)_Q - (K^{-1}\psi_z, q) + \theta (K^{-1}\Pi z, q)}{\|q\|_{\operatorname{div}}} \leq Ch\|z\|_1 + \|\phi_z\|. \end{aligned} \quad (6.44)$$

Therefore, we have

$$\begin{aligned}
& \|A^{1/2}(\phi_\sigma(t) + \alpha\phi_p I(t))\|^2 + \|\phi_u(t)\|^2 + \|\phi_\gamma(t)\|^2 + c_0\|\phi_p(t)\|^2 + \int_0^t (\|\phi_z(s)\|^2 + \|\phi_p(s)\|^2) ds \\
& \leq \epsilon \int_0^t (\|\phi_\sigma(s)\|^2 + \|\phi_p(s)\|^2 + \|\phi_z(s)\|^2) ds + Ch^2(\|\sigma(t)\|_1^2 + \|p(t)\|_1^2 + \|\gamma(t)\|_1^2), \\
& \quad + Ch^2 \int_0^t (\|\partial_t \sigma(s)\|_1^2 + \|\partial_t p(s)\|_1^2 + \|\partial_t \gamma(s)\|_1^2 + \|z(s)\|_1^2). \quad (6.45)
\end{aligned}$$

Next, we choose $\tau = \phi_\sigma$ in (6.30) and use (6.31)-(??) and (6.35)-(6.37):

$$\begin{aligned}
C\|\phi_\sigma\|^2 & \leq -\alpha(A\phi_p I, \phi_\sigma)_Q - (A(\psi_\sigma + \alpha\psi_p I), \Pi^0 \phi_\sigma) - (\psi_\gamma, \Pi^0 \phi_\sigma) - \theta(A\Pi\sigma, \Pi^0 \phi_\sigma) \\
& \quad - \theta(A\alpha Q^0 p I, \Pi^0 \phi_\sigma) - \theta(Q^1 \gamma, \Pi^0 \phi_\sigma) + (A(\Pi\sigma + \alpha Q^0 p I), \phi_\sigma - \Pi^0 \phi_\sigma)_Q \\
& \quad + (Q^1 \gamma, \phi_\sigma - \Pi^0 \phi_\sigma)_Q \leq Ch^2(\|\sigma\|_1^2 + \|p\|_1^2 + \|\gamma\|_1^2) + C\|\phi_p\|^2 + \epsilon\|\phi_\sigma\|^2,
\end{aligned}$$

where in the last step we used (6.6)-(6.8) and Lemma 6.3. Thus, we have

$$\int_0^t \|\phi_\sigma(s)\|^2 ds \leq C \int_0^t h^2(\|\sigma(s)\|_1^2 + \|p(s)\|_1^2 + \|\gamma(s)\|_1^2) ds + C \int_0^t \|\phi_p(s)\|^2 ds. \quad (6.46)$$

On the other hand, it follows from (6.41)-(6.42) and (6.46) that

$$\int_0^t (\|\phi_u(s)\| + \|\phi_\gamma(s)\|) ds \leq C \int_0^t (h(\|\sigma(s)\|_1 + \|p(s)\|_1 + \|\gamma(s)\|_1) + \|\phi_\sigma(s)\| + \|\phi_p(s)\|) ds. \quad (6.47)$$

Combining (6.45)-(6.47), we obtain

$$\begin{aligned}
& \|A^{1/2}(\phi_\sigma(t) + \alpha\phi_p I(t))\|^2 + \|\phi_u(t)\|^2 + \|\phi_\gamma(t)\|^2 + c_0\|\phi_p(t)\|^2 \\
& \quad + \int_0^t (\|\phi_z(s)\|^2 + \|\phi_p(s)\|^2 + \|\phi_\sigma(s)\|^2 + \|\phi_u(s)\|^2 + \|\phi_\gamma(s)\|^2) ds \\
& \leq \epsilon \int_0^t (\|\phi_\sigma(s)\|^2 + \|\phi_p(s)\|^2 + \|\phi_z(s)\|^2) ds + Ch^2(\|\sigma(t)\|_1^2 + \|p(t)\|_1^2 + \|\gamma(t)\|_1^2), \\
& \quad + Ch^2 \int_0^t (\|\sigma(s)\|_1^2 + \|\partial_t \sigma(s)\|_1^2 + \|p(s)\|_1^2 + \|\partial_t p(s)\|_1^2 + \|\gamma(s)\|_1^2 + \|\partial_t \gamma(s)\|_1^2 + \|z(s)\|_1^2). \quad (6.48)
\end{aligned}$$

Choosing ϵ small enough, we get

$$\begin{aligned}
& \|A^{1/2}(\phi_\sigma(t) + \alpha\phi_p I(t))\|^2 + \|\phi_u(t)\|^2 + \|\phi_\gamma(t)\|^2 + c_0\|\phi_p(t)\|^2 \\
& \quad + \int_0^t (\|\phi_z(s)\|^2 + \|\phi_p(s)\|^2 + \|\phi_\sigma(s)\|^2 + \|\phi_u(s)\|^2 + \|\phi_\gamma(s)\|^2) ds \\
& \leq Ch^2(\|\sigma(t)\|_1^2 + \|p(t)\|_1^2 + \|\gamma(t)\|_1^2), \\
& \quad + Ch^2 \int_0^t (\|\sigma(s)\|_1^2 + \|\partial_t \sigma(s)\|_1^2 + \|p(s)\|_1^2 + \|\partial_t p(s)\|_1^2 + \|\gamma(s)\|_1^2 + \|\partial_t \gamma(s)\|_1^2 + \|z(s)\|_1^2). \quad (6.49)
\end{aligned}$$

Step 2: $H(\text{div})$ in space estimate for stress and velocity:

Estimate for stress error follows immediately due to (6.31).

It follows from (6.33) that

$$\|\text{div } \phi_z\| \leq c_0\|\partial_t \phi_p\| + \|\partial_t A^{1/2}(\phi_\sigma + \alpha\phi_p I)\| + Ch(\|\sigma\|_1 + \|\partial_t \sigma\|_1). \quad (6.50)$$

Next we differentiate (6.30)-(6.32), set $\tau = \partial_t \phi_\sigma$, $\xi = \partial_t \phi_\gamma$, $q = \phi_z$, $w = \partial_t \phi_p$ and combine (6.30)-(6.33):

$$\begin{aligned}
& \frac{1}{2} \partial_t \|K^{-1/2} \phi_z\|_Q^2 + \|A^{1/2} \partial_t(\phi_\sigma + \alpha\phi_p I)\|_Q^2 + c_0 \|\partial_t \phi_p\|^2 \\
& = - (A \partial_t(\psi_\sigma + \alpha\psi_p I), \Pi^0 \partial_t \phi_\sigma) - (\partial_t \psi_\gamma, \Pi^0 \partial_t \phi_\sigma) - \theta(A \partial_t \Pi \sigma, \Pi^0 \partial_t \phi_\sigma + \alpha \partial_t \phi_p I) \\
& \quad + (A \partial_t(\Pi \sigma + \alpha Q^0 p I), \partial_t \phi_\sigma - \Pi^0 \partial_t \phi_\sigma)_Q - \theta(\partial_t Q^1 \gamma, \partial_t \Pi^0 \phi_\sigma) + (\partial_t Q^1 \gamma, \partial_t \phi_\sigma - \Pi^0 \partial_t \phi_\sigma)_Q \\
& \quad - (K^{-1} \psi_z, \Pi^0 \partial_t \phi_z) - \theta(K^{-1} \Pi z, \partial_t \Pi^0 \phi_z) + (K^{-1} \Pi z, \partial_t \phi_z - \partial_t \Pi^0 \phi_z)_Q - \alpha(\partial_t \text{tr}(A \psi_\sigma), \partial_t \phi_p) \\
& \quad - \alpha^2(\partial_t \text{tr}(A \psi_p I), \partial_t \phi_p) - \alpha \theta(\partial_t A Q^0 p, \partial_t \Pi^0 \phi_\sigma + \alpha \partial_t \phi_p). \quad (6.51)
\end{aligned}$$

For all terms not corresponding to error in Darcy velocity, we repeat the arguments from (6.34)-(6.38), combining stress and pressure errors into one.

$$\begin{aligned}
& \left| -\theta (A\partial_t \Pi \sigma, \Pi^0 \partial_t \phi_\sigma + \alpha \partial_t \phi_p I) - \theta (\partial_t Q^1 \gamma, \partial_t \Pi^0 \phi_\sigma) - \alpha \theta (\partial_t A Q^0 p, \partial_t \Pi^0 \phi_\sigma + \alpha \partial_t \phi_p) \right| \\
&= \left| \sum_{E \in \mathcal{T}_h} \left(\theta (A\partial_t \Pi \sigma, \Pi^0 \partial_t (\phi_\sigma + \alpha \phi_p I))_E + \theta (\partial_t Q^1 \gamma, \Pi^0 \partial_t (\phi_\sigma + \alpha \phi_p I))_E \right. \right. \\
&\quad \left. \left. + \alpha \theta (\partial_t A Q^0 p, \Pi^0 \partial_t (\phi_\sigma + \alpha \phi_p I))_E \right) \right| \\
&\leq Ch^2 (\|\partial_t \sigma\|_1^2 + \|\partial_t p\|_1^2 + \|\partial_t \gamma\|_1^2) + \epsilon \|\Pi^0 \partial_t \phi_\sigma + \alpha \partial_t \phi_p I\|^2,
\end{aligned} \tag{6.52}$$

where we used the fact that on every $E \in \mathcal{T}_h$, $\phi_p I|_E \in \mathbb{X}_h^0(E)$ and that it is symmetric. Similarly,

$$\begin{aligned}
& \left| - (A\partial_t (\psi_\sigma + \alpha \psi_p I), \Pi^0 \partial_t \phi_\sigma) - (\partial_t \psi_\gamma, \Pi^0 \partial_t \phi_\sigma) - \alpha (\partial_t \text{tr}(A\psi_\sigma), \partial_t \phi_p) - \alpha^2 (\partial_t \text{tr}(A\psi_p I), \partial_t \phi_p) \right| \\
&= \left| - (A\partial_t (\psi_\sigma + \alpha \psi_p I), \partial_t (\Pi^0 \phi_\sigma + \alpha \phi_p)) - (\partial_t \psi_\gamma, \partial_t (\Pi^0 \phi_\sigma + \alpha \phi_p)) \right| \\
&= \left| \sum_{E \in \mathcal{T}_h} \left((A\partial_t (\psi_\sigma + \alpha \psi_p I), \partial_t \Pi^0 (\phi_\sigma + \alpha \phi_p))_E + (\partial_t \psi_\gamma, \partial_t \Pi^0 (\phi_\sigma + \alpha \phi_p))_E \right) \right| \\
&\leq Ch^2 (\|\partial_t \sigma\|_1^2 + \|\partial_t p\|_1^2 + \|\partial_t \gamma\|_1^2) + \epsilon \|\partial_t \phi_\sigma + \alpha \partial_t \phi_p I\|^2,
\end{aligned} \tag{6.54}$$

and

$$\begin{aligned}
& \left| (A\partial_t (\Pi \sigma + \alpha Q^0 p I), \partial_t \phi_\sigma - \Pi^0 \partial_t \phi_\sigma)_Q + (\partial_t Q^1 \gamma, \partial_t \phi_\sigma - \Pi^0 \partial_t \phi_\sigma)_Q \right| \\
&= \left| \sum_{E \in \mathcal{T}_h} \left((A\partial_t (\Pi \sigma + \alpha Q^0 p I), \partial_t (\phi_\sigma + \phi_p I) - \Pi^0 \partial_t (\phi_\sigma + \phi_p I))_{Q,E} \right. \right. \\
&\quad \left. \left. + (\partial_t Q^1 \gamma, \partial_t (\phi_\sigma + \phi_p I) - \Pi^0 \partial_t (\phi_\sigma + \phi_p I))_{E,Q} \right) \right| \\
&\leq Ch^2 (\|\partial_t \sigma\|_1^2 + \|\partial_t p\|_1^2 + \|\partial_t \gamma\|_1^2) + \epsilon \|\partial_t \phi_\sigma + \alpha \partial_t \phi_p I\|^2.
\end{aligned} \tag{6.55}$$

Combining (6.51)-(6.55), we obtain

$$\begin{aligned}
& \|K^{-1/2} \phi_z(t)\|_Q^2 + \int_0^t \left(\|A^{1/2} \partial_t (\phi_\sigma(s) + \alpha \phi_p I(s))\|_Q^2 + c_0 \|\partial_t \phi_p(s)\|^2 \right) ds \\
&\leq C \left(\|K^{-1/2} \phi_z(0)\|_Q^2 + \epsilon \int_0^t \|\partial_t \phi_\sigma(s) + \alpha \partial_t \phi_p(s) I\|^2 ds \right. \\
&\quad + Ch^2 \int_0^t (\|\partial_t \sigma(s)\|_1^2 + \|\partial_t p(s)\|_1^2 + \|\partial_t \gamma(s)\|_1^2) ds \\
&\quad \left. + \int_0^t \left(- (K^{-1} \psi_z(s), \Pi^0 \partial_t \phi_z(s)) - \theta (K^{-1} \Pi z(s), \partial_t \Pi^0 \phi_z(s)) \right. \right. \\
&\quad \left. \left. + (K^{-1} \Pi z(s), \partial_t \phi_z(s) - \partial_t \Pi^0 \phi_z(s))_Q \right) ds \right).
\end{aligned} \tag{6.56}$$

We integrate by parts the terms involving error in Darcy velocity

$$\begin{aligned}
& \int_0^t \left(- (K^{-1} \psi_z(s), \Pi^0 \partial_t \phi_z(s)) - \theta (K^{-1} \Pi z(s), \partial_t \Pi^0 \phi_z(s)) + (K^{-1} \Pi z(s), \partial_t \phi_z(s) - \partial_t \Pi^0 \phi_z(s))_Q \right) ds \\
&= - (K^{-1} \psi_z(t), \Pi^0 \phi_z(t)) - \theta (K^{-1} \Pi z(t), \Pi^0 \phi_z(t)) + (K^{-1} \Pi z(t), \phi_z(t) - \Pi^0 \phi_z(t))_Q \\
&\quad + (K^{-1} \psi_z(0), \Pi^0 \phi_z(0)) + \theta (K^{-1} \Pi z(0), \Pi^0 \phi_z(0)) + (K^{-1} \Pi z(0), \phi_z(0) - \Pi^0 \phi_z(0))_Q \\
&\quad - \int_0^t \left(- (K^{-1} \partial_t \psi_z(s), \Pi^0 \phi_z(s)) - \theta (K^{-1} \partial_t \Pi z(s), \Pi^0 \phi_z(s)) \right. \\
&\quad \left. + (K^{-1} \partial_t \Pi z(s), \phi_z(s) - \Pi^0 \phi_z(s))_Q \right) ds
\end{aligned}$$

Choosing $z_h(0) = \Pi z(0)$, we obtain

$$(K^{-1}\psi_z(0), \Pi^0\phi_z(0)) + \theta (K^{-1}\Pi z(0), \Pi^0\phi_z(0)) + (K^{-1}\Pi z(0), \phi_z(0) - \Pi^0\phi_z(0))_Q = 0, \quad (6.57)$$

and for the rest of the terms we use (6.8), (6.16) and (6.20):

$$\begin{aligned} & - (K^{-1}\psi_z(t), \Pi^0\phi_z(t)) - \theta (K^{-1}\Pi z(t), \Pi^0\phi_z(t)) + (K^{-1}\Pi z(t), \phi_z(t) - \Pi^0\phi_z(t))_Q \\ & - \int_0^t \left(- (K^{-1}\partial_t\psi_z(s), \Pi^0\phi_z(s)) - \theta (K^{-1}\partial_t\Pi z(s), \Pi^0\phi_z(s)) \right. \\ & \quad \left. + (K^{-1}\partial_t\Pi z(s), \phi_z(s) - \Pi^0\phi_z(s))_Q \right) ds \\ & \leq C(h^2\|z(t)\|_1^2 + \epsilon\|\phi_z(t)\|^2) + \int_0^t (h^2\|\partial_t z(s)\|_1^2 + \epsilon\|\phi_z(s)\|^2) ds. \end{aligned} \quad (6.58)$$

From (6.56)-(6.58) we obtain:

$$\begin{aligned} & \|K^{-1/2}\phi_z(t)\|_Q^2 + \int_0^t \left(\|A^{1/2}\partial_t(\phi_\sigma(s) + \alpha\phi_p I(s))\|_Q^2 + c_0\|\partial_t\phi_p(s)\|^2 \right) ds \\ & \leq C(h^2\|z(t)\|_1^2 + \epsilon\|\phi_z(t)\|^2) + C \int_0^t (h^2(\|\partial_t z(s)\|_1^2 + h^2\|\partial_t\sigma(s)\|_1^2 + \epsilon\|\phi_z(s)\|^2) ds.. \end{aligned} \quad (6.59)$$

Combining (6.59), (6.56), (6.44) and using the equivalence of norms, we get

$$\begin{aligned} & \|\phi_z(t)\|^2 + \|\phi_p(t)\|^2 + \int_0^t (\|\partial_t(\phi_\sigma(s) + \alpha\phi_p I(s))\|^2 + c_0\|\partial_t\phi_p(s)\|^2) ds \\ & \leq C \int_0^t h^2(\|\partial_t z(s)\|_1^2 + \|\partial_t\sigma(s)\|_1^2 + \|\partial_t p(s)\|_1^2 + \|\partial_t\gamma(s)\|_1^2) ds \\ & \quad + \epsilon \int_0^t (\|\phi_z(s)\|^2 + \|\partial_t(\phi_\sigma(s) + \alpha\phi_p I(s))\|^2) ds + C(h^2\|z(t)\|_1^2 + \epsilon\|\phi_z(t)\|^2). \end{aligned} \quad (6.60)$$

Hence, (6.50) and (6.60) yield

$$\begin{aligned} & \|\phi_z(t)\|^2 + \|\phi_p(t)\|^2 + \int_0^t \|\operatorname{div} \phi_z\|^2 ds \\ & \leq \epsilon \int_0^t \|\phi_z(s)\|^2 ds \\ & \quad + C \left(\int_0^t h^2(\|\partial_t z(s)\|_1^2 + \|\sigma(s)\|_1^2 + \|\partial_t\sigma(s)\|_1^2 + \|\partial_t p(s)\|_1^2 + \|\partial_t\gamma(s)\|_1^2) ds + \|z(t)\|_1^2 \right). \end{aligned} \quad (6.61)$$

Step 3: obtaining the final result:

We note that

$$\begin{aligned} \|\phi_\sigma\| & \leq C\|A^{1/2}\phi_\sigma\| \leq C \left(\|A^{1/2}(\phi_\sigma + \alpha\phi_p I)\| + \|A^{1/2}\alpha\phi_p I\| \right) \\ & \leq C \left(\|A^{1/2}(\phi_\sigma + \alpha\phi_p I)\| + \|\phi_p\| \right). \end{aligned} \quad (6.62)$$

Therefore, combining (6.49), (6.61) and (6.62), we obtain the following result.

Theorem 6.1. *Let $(\sigma_h, u_h, \gamma_h, z_h, p_h) \in \mathbb{X}_h \times V_h \times \Theta_h \times Z_h \times W_h$ be the solution of (3.12)-(3.16) and $(\sigma, u, \gamma, z, p) \in \mathbb{X} \times V \times \mathbb{Q} \times Z \times W \cap H^1(0, T; (H^1(\Omega))^{d \times d}) \times H^1(0, T; (H^1(\Omega))^d) \times H^1(0, T; H^1(\Omega)^{d \times d, skew}) \times H^1(0, T; (H^1(\Omega))^d) \times H^1(0, T; H^1(\Omega))$ be the solution of (2.8)-(2.12). Then*

the following error estimate holds:

$$\begin{aligned}
& \|\sigma - \sigma_h\|_{L^\infty(0,T;H(\text{div},\Omega))} + \|u - u_h\|_{L^\infty(0,T;L^2(\Omega))} + \|\gamma - \gamma_h\|_{L^\infty(0,T;L^2(\Omega))} + \|z - z_h\|_{L^\infty(0,T;L^2(\Omega))} \\
& + \|p - p_h\|_{L^\infty(0,T;L^2(\Omega))} + \|\sigma - \sigma_h\|_{L^2(0,T;H(\text{div},\Omega))} + \|u - u_h\|_{L^2(0,T;L^2(\Omega))} + \|\gamma - \gamma_h\|_{L^2(0,T;L^2(\Omega))} \\
& + \|z - z_h\|_{L^2(0,T;H(\text{div},\Omega))} + \|p - p_h\|_{L^2(0,T;L^2(\Omega))} \\
& \leq Ch \left(\|s\|_{H^1(0,T;H^1(\Omega))} + \|u\|_{L^2(0,T;H^1(\Omega))} + \|\gamma\|_{H^1(0,T;H^1(\Omega))} + \|z\|_{H^1(0,T;H^1(\Omega))} \right. \\
& + \|p\|_{H^1(0,T;H^1(\Omega))} + \|\sigma\|_{L^\infty(0,T;H^1(\Omega))} + \|u\|_{L^\infty(0,T;L^2(\Omega))} \\
& \left. + \|\gamma\|_{L^\infty(0,T;H^1(\Omega))} + \|z\|_{L^\infty(0,T;H^1(\Omega))} + \|p\|_{L^\infty(0,T;H^1(\Omega))} \right). \tag{6.63}
\end{aligned}$$

7 Fully-discrete MSMFE-MFMFE method

In this section we present the fully-discrete method based on the backward Euler time discretization and show how the algebraic system at each time step can be reduced to a symmetric and positived definite cell-centered displacement-pressure system.

Let $0 = t_0 < t_1 < \dots < t_N = T$ be a partition of the time interval $[0, T]$ with time steps $\Delta t_n = t_n - t_{n-1}$, $n = 1, \dots, N$. Let $\varphi^n = \varphi(t_n)$ and $\partial_t^n \varphi = (\varphi^n - \varphi^{n-1})/\Delta t_n$. The fully-discrete MSMFE-MFMFE method is: given σ_h^0 and p_h^0 , for $n = 1, \dots, N$, find $(\sigma_h^n, u_h^n, \gamma_h^n, z_h^n, p_h^n) \in \mathbb{X}_h \times V_h \times \mathbb{Q}_h \times Z_h \times W_h$ such that

$$(A(\sigma_h^n + \alpha p_h^n I), \tau)_Q + (u_h^n, \text{div } \tau) + (\gamma_h^n, \tau)_Q = 0, \quad \forall \tau \in \mathbb{X}_h, \tag{7.1}$$

$$-(\text{div } \sigma_h^n, v) = (f^n, v), \quad \forall v \in V_h, \tag{7.2}$$

$$(\sigma_h^n, \xi)_Q = 0, \quad \forall \xi \in \mathbb{Q}_h, \tag{7.3}$$

$$(K^{-1} z_h^n, \zeta)_Q - (p_h^n, \text{div } \zeta) = 0 \quad \forall \zeta \in Z_h, \tag{7.4}$$

$$c_0 (\partial_t^n p_h, w) + \alpha (\partial_t^n A(\sigma_h + \alpha p_h I), wI)_Q + (\text{div } z_h^n, w) = (q^n, w), \quad \forall w \in W_h. \tag{7.5}$$

Lemma 7.1. *The fully discrete method (7.1)–(7.5) has a unique solution.*

Proof. TODO: The proof follows from the proof of the range condition in Lemma 4.1. \square

7.1 Reduction to a cell-centered displacement-pressure system

The choice of trapezoidal quadrature rule implies that on each element, the stress and velocity degrees of freedom associated with a vertex become decoupled from the rest of the degrees of freedom. As a result, the assembled velocity mass matrix in (3.15) has a block-diagonal structure with one block per grid vertex. The dimensions of each velocity block equals the number of velocity DOFs associated with the vertex. For example, this dimension is 4 for logically rectangular quadrilateral grids. Inverting each local block in mass matrix in (3.15) allows for expressing the velocity DOF associated with a vertex in terms of the pressures at the centers of the elements that share the vertex.

Similarly, inverting each local block in mass matrix in (3.12) allows for expressing the stress DOF associated with a vertex in terms of the corresponding displacements, rotations and pressures. By substituting these expressions into equations (3.13)–(3.14) one gets the intermediate step, where the elasticity system was reduced to a cell-centered displacement-rotation system. Due to the choice of the quadrature rule, the rotation basis functions corresponding to each vertex of the grid become decoupled from the rest of the variables other than the stress DOF at this same vertex, leading to matrix $A_{\sigma\gamma} A_{\sigma\sigma}^{-1} A_{\sigma\gamma}^T$ being diagonal (see [3, 4]). With this, one obtains the expression for the rotation DOF in terms of the displacements and pressures, which can be further substituted into (3.13) leading to a final displacement-pressure system.

More precisely, in matrix form we have

$$\begin{aligned}
& \begin{pmatrix} A_{\sigma\sigma} & A_{\sigma u}^T & A_{\sigma\gamma}^T & 0 & A_{\sigma p}^T \\ -A_{\sigma u} & 0 & 0 & 0 & 0 \\ -A_{\sigma\gamma} & 0 & 0 & 0 & 0 \\ 0 & 0 & 0 & A_{zz} & A_{zp}^T \\ A_{\sigma p} & 0 & 0 & -A_{zp} & A_{pp} \end{pmatrix} \begin{pmatrix} \sigma \\ u \\ \gamma \\ z \\ p \end{pmatrix} \\
& \xrightarrow{\sigma = -A_{\sigma\sigma}^{-1} A_{\sigma u}^T u - A_{\sigma\sigma}^{-1} A_{\sigma\gamma}^T \gamma - A_{\sigma\sigma}^{-1} A_{\sigma p}^T p} \begin{pmatrix} A_{\sigma u} A_{\sigma\sigma}^{-1} A_{\sigma u}^T & A_{\sigma u} A_{\sigma\sigma}^{-1} A_{\sigma\gamma}^T & 0 & A_{\sigma u} A_{\sigma\sigma}^{-1} A_{\sigma p}^T \\ A_{\sigma\gamma} A_{\sigma\sigma}^{-1} A_{\sigma u}^T & A_{\sigma\gamma} A_{\sigma\sigma}^{-1} A_{\sigma\gamma}^T & 0 & A_{\sigma\gamma} A_{\sigma\sigma}^{-1} A_{\sigma p}^T \\ 0 & 0 & A_{zz} & A_{zp}^T \\ -A_{\sigma p} A_{\sigma\sigma}^{-1} A_{\sigma u}^T & -A_{\sigma p} A_{\sigma\sigma}^{-1} A_{\sigma\gamma}^T & -A_{zp} & A_{pp} - A_{\sigma p} A_{\sigma\sigma}^{-1} A_{\sigma p}^T \end{pmatrix} \begin{pmatrix} u \\ \gamma \\ z \\ p \end{pmatrix} \\
& \xrightarrow{z = -A_{zz}^{-1} A_{zp}^T p} \begin{pmatrix} A_{u\sigma u} & A_{u\sigma\gamma} & A_{u\sigma p} \\ A_{u\sigma\gamma}^T & A_{\gamma\sigma\gamma} & A_{\gamma\sigma p} \\ -A_{u\sigma p}^T & -A_{\gamma\sigma p}^T & A_{p\sigma zp} \end{pmatrix} \begin{pmatrix} u \\ \gamma \\ p \end{pmatrix} \\
& \xrightarrow{\gamma = -A_{\gamma\sigma\gamma}^{-1} A_{\gamma\sigma p} p - A_{\gamma\sigma\gamma}^{-1} A_{u\sigma\gamma}^T u} \begin{pmatrix} A_{u\sigma u} - A_{u\sigma\gamma} A_{\gamma\sigma\gamma}^{-1} A_{u\sigma\gamma}^T & A_{u\sigma p} - A_{u\sigma\gamma} A_{\gamma\sigma\gamma}^{-1} A_{\gamma\sigma p} \\ -A_{u\sigma p}^T + A_{u\sigma\gamma}^T A_{\gamma\sigma\gamma}^{-1} A_{\gamma\sigma p}^T & A_{p\sigma zp} + A_{\gamma\sigma p}^T A_{\gamma\sigma\gamma}^{-1} A_{\gamma\sigma p} \end{pmatrix} \begin{pmatrix} u \\ p \end{pmatrix}.
\end{aligned}$$

And finally, the displacement-pressure system for the Biot poroelasticity model reads as follows

$$\begin{pmatrix} A_{u\sigma u} - A_{u\sigma\gamma} A_{\gamma\sigma\gamma}^{-1} A_{u\sigma\gamma}^T & A_{u\sigma p} - A_{u\sigma\gamma} A_{\gamma\sigma\gamma}^{-1} A_{\gamma\sigma p} \\ -A_{u\sigma p}^T + A_{u\sigma\gamma}^T A_{\gamma\sigma\gamma}^{-1} A_{\gamma\sigma p}^T & A_{p\sigma zp} + A_{\gamma\sigma p}^T A_{\gamma\sigma\gamma}^{-1} A_{\gamma\sigma p} \end{pmatrix} \begin{pmatrix} u \\ p \end{pmatrix} = \begin{pmatrix} F_u \\ F_p \end{pmatrix} \quad (7.6)$$

where

$$\begin{aligned}
A_{u\sigma u} &:= A_{\sigma u} A_{\sigma\sigma}^{-1} A_{\sigma u}^T, & A_{u\sigma\gamma} &:= A_{\sigma u} A_{\sigma\sigma}^{-1} A_{\sigma\gamma}^T, \\
A_{\gamma\sigma\gamma} &:= A_{\sigma\gamma} A_{\sigma\sigma}^{-1} A_{\sigma\gamma}^T, & A_{u\sigma p} &:= A_{\sigma u} A_{\sigma\sigma}^{-1} A_{\sigma p}^T, \\
A_{\gamma\sigma p} &:= A_{\sigma\gamma} A_{\sigma\sigma}^{-1} A_{\sigma p}^T, & A_{p\sigma zp} &:= A_{pp} - A_{\sigma p} A_{\sigma\sigma}^{-1} A_{\sigma p}^T + A_{zp} A_{\sigma\sigma}^{-1} A_{zp}^T,
\end{aligned}$$

and F_u, F_p are the right-hand side functions transformed accordingly to the procedure above.

Lemma 7.2. *The cell-centered finite difference system for the displacement and pressure obtained from (3.12)-(3.16) using the procedure described above is symmetric and positive definite.*

Proof. The proof follows from the inf-sup conditions for the MSMFE and MFMFE methods, Corollary 3.1 and the combined stress-pressure coercivity estimate, see [43, 3, 4] for details. \square

8 Numerical results

In this section we provide several numerical tests verifying the theoretically predicted convergence rates and illustrating the behavior of the proposed method on simplicial and quadrilateral grids. We also briefly address the issue of locking when dealing with small storativity coefficients.

8.1 Example 1

We first verify the method's convergence on simplicial grids in 3 dimensions. For this, we use a unit cube as a computational domain, and choose the analytical solution for pressure and displacement as follows:

$$p = \cos(t)(x + y + z + 1.5), \quad u = \sin(t) \begin{pmatrix} -0.1(e^x - 1) \sin(\pi x) \sin(\pi y) \\ -(e^x - 1)(y - \cos(\frac{\pi}{12}))(y - 0.5) + \sin(\frac{\pi}{12})(z - 0.5) - 0.5 \\ -(e^x - 1)(z - \sin(\frac{\pi}{12}))(y - 0.5) - \cos(\frac{\pi}{12})(z - 0.5) - 0.5 \end{pmatrix}.$$

The permeability tensor is of the form

$$K = \begin{pmatrix} x^2 + y^2 + 1 & 0 & 0 \\ 0 & z^2 + 1 & \sin(xy) \\ 0 & \sin(xy) & x^2 y^2 + 1 \end{pmatrix},$$

Parameter	Symbol	Values
Lame coefficient	μ	100.0
Lame coefficient	λ	100.0
Mass storativity	c_0	1.0
Biot-Willis constant	α	1.0
Total time	T	10^{-3}
Time step	Δt	10^{-4}

Table 1: Physical parameters, Examples 1 and 2

and the rest of the parameters are presented in Table 1.

Using the analytical solution provided above and equations (2.3)-(2.4) we recover the rest of variables and right-hand side functions. Dirichlet boundary conditions for the pressure and the displacement are specified on the entire boundary of the domain.

h	$\ \sigma - \sigma_h\ _{L^2(0,T;L^2(\Omega))}$		$\ \operatorname{div}(\sigma - \sigma_h)\ _{L^2(0,T;L^2(\Omega))}$		$\ u - u_h\ _{L^2(0,T;L^2(\Omega))}$	
	error	rate	error	rate	error	rate
1/4	3.07E-02	-	2.29E-01	-	8.54E-01	-
1/8	9.92E-03	1.6	1.14E-01	1.0	2.32E-01	1.9
1/16	4.90E-03	1.0	5.68E-02	1.0	7.44E-02	1.6
1/32	2.50E-03	1.0	2.84E-02	1.0	2.97E-02	1.3
h	$\ \gamma - \gamma_h\ _{L^2(0,T;L^2(\Omega))}$		$\ z - z_h\ _{L^2(0,T;L^2(\Omega))}$		$\ \operatorname{div}(z - z_h)\ _{L^2(0,T;L^2(\Omega))}$	
	error	rate	error	rate	error	rate
1/4	7.65E-01	-	1.06E-02	-	5.85E-02	-
1/8	2.32E-01	1.7	2.66E-03	2.0	2.31E-02	1.3
1/16	7.00E-02	1.7	6.64E-04	2.0	7.70E-03	1.6
1/32	2.12E-02	1.7	1.66E-04	2.0	2.71E-03	1.5
h	$\ p - p_h\ _{L^2(0,T;L^2(\Omega))}$		$\ \sigma - \sigma_h\ _{L^\infty(0,T;L^2(\Omega))}$		$\ p - p_h\ _{L^\infty(0,T;L^2(\Omega))}$	
	error	rate	error	rate	error	rate
1/4	1.92E-04	-	2.29E-01	-	2.18E-04	-
1/8	5.56E-05	1.8	1.14E-01	1.0	6.39E-05	1.8
1/16	1.28E-05	2.1	5.70E-02	1.0	1.30E-05	2.3
1/32	2.55E-06	2.3	2.85E-02	1.0	2.78E-06	2.2

Table 2: Example 1, computed numerical errors and convergence rates.

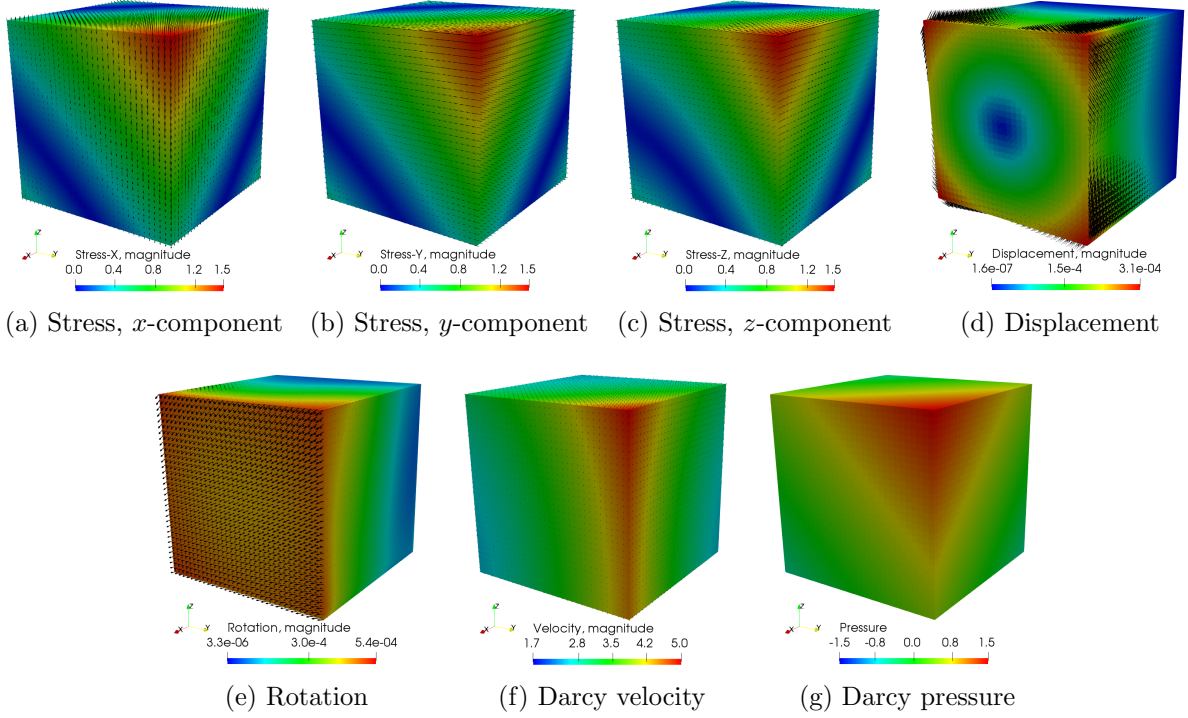


Figure 1: Example 1, computed solution at the final time step.

In Table 2 we present computed relative errors and rates for this example. For the sake of space we report only the errors that would normally be of interest in studying the behavior of this problem. As one can observe, the results agree with theory of the previous section.

8.2 Example 2

The second test case is to study the convergence of the method on an h^2 -parallelogram grid. We consider the following analytical solution

$$p = \exp(t)(\sin(\pi x) \cos(\pi y) + 10), \quad u = \exp(t) \left(\frac{x^3 y^4 + x^2 + \sin((1-x)(1-y)) \cos(1-y)}{(1-x)^4 (1-y)^3 + (1-y)^2 + \cos(xy) \sin(x)} \right).$$

and the permeability tensor of the form

$$\begin{pmatrix} (x+1)^2 + y^2 & \sin(xy) \\ \sin(xy) & (x+1)^2 \end{pmatrix}.$$

The Poisson ratio is set to be $\nu = 0.2$ and Young's modulus varies over the domain as $E = \sin(5\pi x) \sin(5\pi y) + 5$. The Lamé parameters are then computed using the well known relations

$$\lambda = \frac{E\nu}{(1+\nu)(1-2\nu)}, \quad \mu = \frac{E}{2(1+\nu)}.$$

The time discretization parameters are the same as in Table 1.

The computational grid for this case is obtained by taking a unit square with initial partitioning into a mesh with $h = \frac{1}{4}$, and further transforming it by the following map (see Figure 2):

$$x = \hat{x} + 0.03 \cos(3\pi \hat{x}) \cos(3\pi \hat{y}), \quad y = \hat{y} - 0.04 \cos(3\pi \hat{x}) \cos(3\pi \hat{y}).$$

As in the previous test case we observe optimal convergence rates for all variables in their respective norms.

h	$\ \sigma - \sigma_h\ _{L^2(0,T;L^2(\Omega))}$ error	rate	$\ \operatorname{div}(\sigma - \sigma_h)\ _{L^2(0,T;L^2(\Omega))}$ error	rate	$\ u - u_h\ _{L^2(0,T;L^2(\Omega))}$ error	rate
1/8	6.505e-02	-	4.305e-01	-	7.985e-02	-
1/16	3.130e-02	1.1	2.336e-01	0.9	3.959e-02	1.0
1/32	1.506e-02	1.1	1.172e-01	1.0	1.975e-02	1.0
1/64	7.435e-03	1.0	5.856e-02	1.0	9.869e-03	1.0
1/128	3.709e-03	1.0	2.927e-02	1.0	4.934e-03	1.0
h	$\ \gamma - \gamma_h\ _{L^2(0,T;L^2(\Omega))}$ error	rate	$\ z - z_h\ _{L^2(0,T;L^2(\Omega))}$ error	rate	$\ \operatorname{div}(z - z_h)\ _{L^2(0,T;L^2(\Omega))}$ error	rate
1/8	1.964e-01	-	5.321e-01	-	2.531e+00	-
1/16	7.444e-02	1.4	2.935e-01	0.9	1.599e+00	0.7
1/32	2.767e-02	1.4	9.757e-02	1.6	5.864e-01	1.5
1/64	1.016e-02	1.5	2.999e-02	1.7	1.767e-01	1.7
1/128	3.697e-03	1.5	1.080e-02	1.5	4.984e-02	1.8
h	$\ p - p_h\ _{L^2(0,T;L^2(\Omega))}$ error	rate	$\ \sigma - \sigma_h\ _{L^\infty(0,T;L^2(\Omega))}$ error	rate	$\ p - p_h\ _{L^\infty(0,T;L^2(\Omega))}$ error	rate
1/8	1.588e-02	-	6.595e-02	-	2.519e-02	-
1/16	6.755e-03	1.2	3.180e-02	1.1	1.170e-02	1.1
1/32	2.647e-03	1.4	1.516e-02	1.1	3.863e-03	1.6
1/64	1.178e-03	1.2	7.449e-03	1.0	1.387e-03	1.5
1/128	5.680e-04	1.1	3.710e-03	1.0	5.973e-04	1.2

Table 3: Example 2, computed numerical errors and convergence rates.

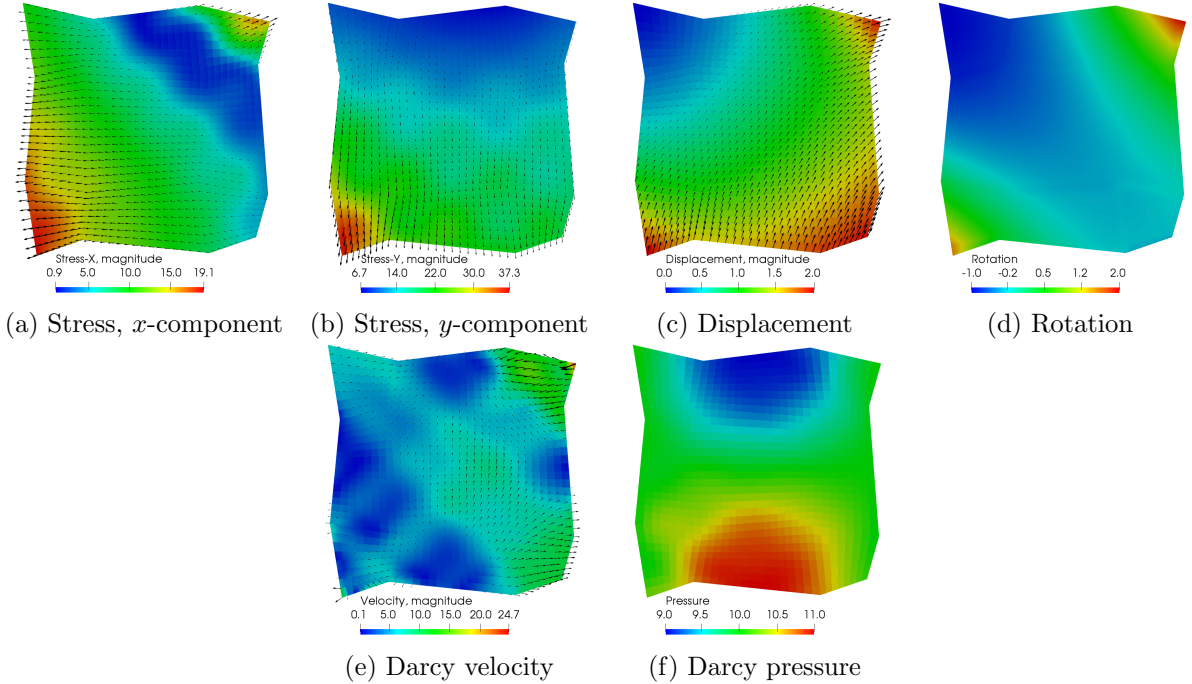


Figure 2: Example 2, computed solution at the final time step.

8.3 Example 3

Our third example is to confirm that the coupled MFMFE-MSMFE method for the Biot system inherits is locking free, due to its mixed nature. It was shown in [32] that with continuous finite elements used for the elasticity part of the system, locking occurs when the storativity coefficient is very small. One of the typical model problems that illustrates such behavior is the cantilever bracket problem [25].

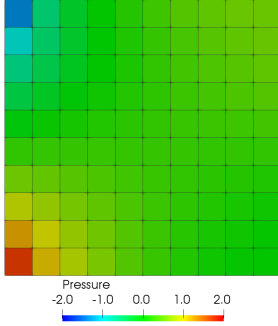
The computational domain is a unit square $[0, 1] \times [0, 1]$. We impose a no-flow boundary condition along all sides, the deformation is fixed along the left edge, and a downward traction is applied at the top of the unit square. The bottom and right sides are enforced to be traction-free. More precisely, with the sides of the domain being labeled as Γ_1 to Γ_4 , going counterclockwise from the bottom side, we have

$$\begin{aligned} z \cdot n &= 0, & \text{on } \partial\Omega = \Gamma_1 \cup \Gamma_2 \cup \Gamma_3 \cup \Gamma_4, \\ \sigma n &= (0, -1)^T, & \text{on } \Gamma_3, \\ \sigma n &= (0, 0)^T, & \text{on } \Gamma_1 \cup \Gamma_2, \\ u &= (0, 0)^T, & \text{on } \Gamma_4. \end{aligned}$$

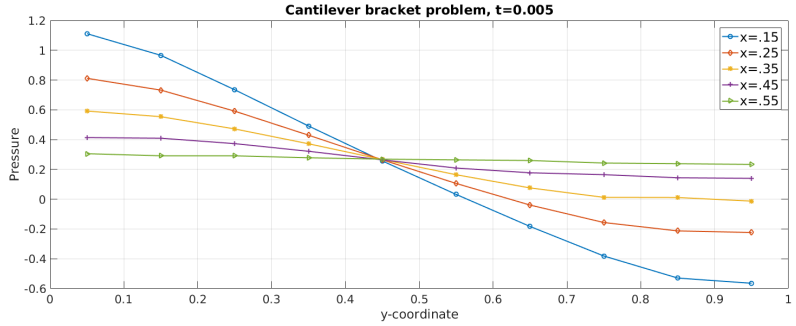
We use the same physical parameters as in [32], as they typically induce locking:

$$E = 10^5, \quad \nu = 0.4, \quad \alpha = 0.93, \quad c_0 = 0, \quad K = 10^{-7},$$

The time step is set to be $\Delta t = 0.001$ and the total simulation time is $T = 1$.



(a) Pressure field, $t = 0.001$.



(b) Pressure along different x -lines, $t = 0.005$.

Figure 3: Example 3, computed pressure solutions.

Figure 3a shows that the coupled MSMFE-MFMFE method yields a smooth pressure field, without a typically arising checkerboard pattern that one obtains with a CG-mixed method for the Biot system (see [32]) on early time steps. In addition, Figure 3b shows the pressure solution along different x -lines at time $t = 0.005$. The latter illustrates the lack of oscillations and that the solution of the coupled mixed method agrees with the one obtained by DG-mixed or stabilized CG-mixed [32, 25]

References

- [1] I. Aavatsmark. An introduction to multipoint flux approximations for quadrilateral grids. *Comput. Geosci.*, 6(3-4):405–432, 2002. Locally conservative numerical methods for flow in porous media.
- [2] I. Aavatsmark, T. Barkve, O. Bøe, and T. Mannseth. Discretization on unstructured grids for inhomogeneous, anisotropic media. I. Derivation of the methods. *SIAM J. Sci. Comput.*, 19(5):1700–1716, 1998.
- [3] I. Ambartsumyan, E. Khattatov, J. Nordbotten, and I. Yotov. A multipoint stress mixed finite element method for elasticity I: Simplicial grids. Preprint.
- [4] I. Ambartsumyan, E. Khattatov, J. Nordbotten, and I. Yotov. A multipoint stress mixed finite element method for elasticity II: Quadrilateral grids. Preprint.
- [5] D. N. Arnold, G. Awanou, and W. Qiu. Mixed finite elements for elasticity on quadrilateral meshes. *Adv. Comput. Math.*, 41(3):553–572, 2015.

- [6] D. N. Arnold, D. Boffi, and R. S. Falk. Quadrilateral $H(\text{div})$ finite elements. *SIAM J. Numer. Anal.*, 42(6):2429–2451, 2005.
- [7] D. N. Arnold, R. S. Falk, and R. Winther. Mixed finite element methods for linear elasticity with weakly imposed symmetry. *Math. Comp.*, 76(260):1699–1723, 2007.
- [8] M. A. Biot. General theory of three-dimensional consolidation. *J. Appl. Phys.*, 12(2):155–164, 1941.
- [9] D. Boffi, F. Brezzi, L. F. Demkowicz, R. G. Durán, R. S. Falk, and M. Fortin. *Mixed finite elements, compatibility conditions, and applications*, volume 1939 of *Lecture Notes in Mathematics*. Springer-Verlag, Berlin; Fondazione C.I.M.E., Florence, 2008. Lectures given at the C.I.M.E. Summer School held in Cetraro, June 26–July 1, 2006, Edited by Boffi and Lucia Gastaldi.
- [10] F. Brezzi, J. Douglas, Jr., and L. D. Marini. Two families of mixed finite elements for second order elliptic problems. *Numer. Math.*, 47(2):217–235, 1985.
- [11] F. Brezzi and M. Fortin. *Mixed and hybrid finite element methods*, volume 15 of *Springer Series in Computational Mathematics*. Springer-Verlag, New York, 1991.
- [12] L. Chin, L. Thomas, J. Sylte, and R. Pierson. Iterative coupled analysis of geomechanics and fluid flow for rock compaction in reservoir simulation. *Oil & Gas Science and Technology*, 57(5):485–497, 2002.
- [13] P. G. Ciarlet. *The finite element method for elliptic problems*. North-Holland Publishing Co., Amsterdam-New York-Oxford, 1978. Studies in Mathematics and its Applications, Vol. 4.
- [14] M. G. Edwards. Unstructured, control-volume distributed, full-tensor finite-volume schemes with flow based grids. *Comput. Geosci.*, 6(3-4):433–452, 2002. Locally conservative numerical methods for flow in porous media.
- [15] M. G. Edwards and C. F. Rogers. Finite volume discretization with imposed flux continuity for the general tensor pressure equation. *Comput. Geosci.*, 2(4):259–290 (1999), 1998.
- [16] R. E. Ewing, O. P. Iliev, R. D. Lazarov, and A. Naumovich. On convergence of certain finite volume difference discretizations for 1D poroelasticity interface problems. *Numer. Methods Partial Differential Equations*, 23(3):652–671, 2007.
- [17] X. Gai. *A coupled geomechanics and reservoir flow model on parallel computers*. PhD thesis, 2004.
- [18] X. Gai, R. H. Dean, M. F. Wheeler, R. Liu, et al. Coupled geomechanical and reservoir modeling on parallel computers. In *SPE Reservoir Simulation Symposium*. Society of Petroleum Engineers, 2003.
- [19] F. J. Gaspar, F. J. Lisbona, and P. N. Vabishchevich. A finite difference analysis of Biot’s consolidation model. *Appl. Numer. Math.*, 44(4):487–506, 2003.
- [20] V. Girault, G. Pencheva, M. F. Wheeler, and T. Wildey. Domain decomposition for poroelasticity and elasticity with dg jumps and mortars. *Math. Mod. Meth. Appl. S.*, 21(01):169–213, 2011.
- [21] R. Ingram, M. F. Wheeler, and I. Yotov. A multipoint flux mixed finite element method on hexahedra. *SIAM J. Numer. Anal.*, 48(4):1281–1312, 2010.
- [22] J. Korsawe and G. Starke. A least-squares mixed finite element method for Biot’s consolidation problem in porous media. *SIAM J. Numer. Anal.*, 43(1):318–339, 2005.
- [23] J. Korsawe, G. Starke, W. Wang, and O. Kolditz. Finite element analysis of poro-elastic consolidation in porous media: standard and mixed approaches. *Comput. Methods Appl. Mech. Engrg.*, 195(9-12):1096–1115, 2006.

- [24] J. J. Lee. Robust error analysis of coupled mixed methods for biots consolidation model. *J. Sci. Comput.*, 69(2):610–632, 2016.
- [25] R. Liu. *Discontinuous Galerkin finite element solution for poromechanics*. PhD thesis, 2004.
- [26] M. A. Murad and A. F. D. Loula. Improved accuracy in finite element analysis of Biot’s consolidation problem. *Comput. Methods Appl. Mech. Engrg.*, 95(3):359–382, 1992.
- [27] M. A. Murad, V. Thomée, and A. F. D. Loula. Asymptotic behavior of semidiscrete finite-element approximations of Biot’s consolidation problem. *SIAM J. Numer. Anal.*, 33(3):1065–1083, 1996.
- [28] J. M. Nordbotten. Convergence of a cell-centered finite volume discretization for linear elasticity. *SIAM J. Numer. Anal.*, 53(6):2605–2625, 2015.
- [29] J. M. Nordbotten. Stable cell-centered finite volume discretization for Biot equations. *SIAM J. Numer. Anal.*, 54(2):942–968, 2016.
- [30] P. J. Phillips and M. F. Wheeler. A coupling of mixed and continuous Galerkin finite element methods for poroelasticity. I. The continuous in time case. *Comput. Geosci.*, 11(2):131–144, 2007.
- [31] P. J. Phillips and M. F. Wheeler. A coupling of mixed and continuous Galerkin finite element methods for poroelasticity. II. The discrete-in-time case. *Comput. Geosci.*, 11(2):145–158, 2007.
- [32] P. J. Phillips and M. F. Wheeler. Overcoming the problem of locking in linear elasticity and poroelasticity: an heuristic approach. *Computat. Geosci.*, 13(1):5, 2009.
- [33] P.-A. Raviart and J. M. Thomas. A mixed finite element method for 2nd order elliptic problems. pages 292–315. *Lecture Notes in Math.*, Vol. 606, 1977.
- [34] J. E. Roberts and J.-M. Thomas. Mixed and hybrid methods. In *Handbook of numerical analysis, Vol. II*, *Handb. Numer. Anal.*, II, pages 523–639. North-Holland, Amsterdam, 1991.
- [35] A. Settari and F. Mourits. Coupling of geomechanics and reservoir simulation models. *Computer Methods and Advances in Geomechanics*, 3:2151–2158, 1994.
- [36] R. E. Showalter. Diffusion in poro-elastic media. *J. Math. Anal. Appl.*, 251(1):310–340, 2000.
- [37] R. E. Showalter. *Monotone operators in Banach space and nonlinear partial differential equations*, volume 49. American Mathematical Soc., 2013.
- [38] J. Wang and T. Mathew. Mixed finite element methods over quadrilaterals. In *Conference on Advances in Numerical Methods and Applications, IT Dimov, B. Sendov, and P. Vassilevski, eds.*, *World Scientific, River Edge, NJ*, pages 203–214, 1994.
- [39] M. F. Wheeler, G. Xue, and I. Yotov. Benchmark 3d: A multipoint flux mixed finite element method on general hexahedra. *Springer Proc. Math.*, 4:1055–1065, 2011.
- [40] M. F. Wheeler, G. Xue, and I. Yotov. A multipoint flux mixed finite element method on distorted quadrilaterals and hexahedra. *Numer. Math.*, 121(1):165–204, 2012.
- [41] M. F. Wheeler, G. Xue, and I. Yotov. A multiscale mortar multipoint flux mixed finite element method. *ESAIM Math. Model. Numer. Anal.*, 46(4):759–796, 2012.
- [42] M. F. Wheeler, G. Xue, and I. Yotov. Coupling multipoint flux mixed finite element methods with continuous galerkin methods for poroelasticity. *Computat. Geosci.*, 18(1):57–75, 2014.
- [43] M. F. Wheeler and I. Yotov. A multipoint flux mixed finite element method. *SIAM J. Numer. Anal.*, 44(5):2082–2106, 2006.